COMBINATION EPIGENETIC THERAPY CAN SENSITIZE OVARIAN CANCER TO IMMUNE CHECKPOINT THERAPY

by
Meredith Stone

A dissertation submitted to Johns Hopkins University in conformity with the requirements
for the degree of Doctor of Philosophy

Baltimore, Maryland

March, 2017

Abstract

While immune checkpoint blockade is approved for other solid tumors, such as non-small cell lung cancer, melanoma, kidney cancer, and bladder cancer, it has not yet been successfully used in ovarian cancer. Ovarian cancer is the leading cause of death from gynecological malignancies in the United States, and new therapies are needed. To study the relationship between the tumor, immune system, and immunotherapy, it is necessary to use an immunocompetent model of ovarian cancer. Therefore, we characterized four related syngeneic epithelial ovarian cell lines, MOSEC, Roby-ID8-luc2, Roby-ID8-nonluc, and ID8-VEGF-defensin, that can form tumors in C57Bl/6 mice and optimized the methods of measuring tumor burden in order to determine drug efficacy. Using the ID8-VEGF-defensin cell line, which grew the most quickly in mice, we have shown that combination epigenetic therapy improves tumor response to immune checkpoint blockade, including decreasing tumor burden and extending the survival of the mice. One epigenetic drug used, the demethylating agent 5-azacytidine (AZA), triggers immune gene upregulation, apoptosis, and cell cycle arrest in the tumor cells. AZA pre-treatment of tumor cells that are then injected into mice increases the number of immune cells in the tumor microenvironment and decreases tumor burden. In contrast, a combination of AZA and a histone deacetylase inhibitor is only effective when the tumor and an intact immune system are treated together, indicating that the combination has specific effects on immune cells. These include an increase in the percentage of activated T and NK cells, and a decrease in the number of macrophages in the tumor microenvironment. Furthermore, the combination therapy of AZA and the HDACi Givinostat sensitizes the tumors to immune checkpoint blockade (α-PD-1). Finally, the type I interferon signaling that is triggered in the tumor cells by AZA is important in the immune and tumor responses, because when the interferon-α receptor is blocked *in vivo*, the effects of AZA on tumor burden, survival, and some of the immune cells are rescued. In conclusion, combination epigenetic therapy affects both the tumor cells and the immune cells in the tumor microenvironment to sensitize ovarian cancer tumors to α-PD-1.

Thesis Readers

Cynthia Zahnow, Ph.D.

Associate Professor of Oncology, The Sidney Kimmel Comprehensive Cancer Center at Johns Hopkins

Stephen Baylin, M.D.

Professor of Oncology, The Sidney Kimmel Comprehensive Cancer Center at Johns Hopkins

Acknowledgements

Table of Contents

List of Abbreviations

MOSEC	Mouse ovarian surface epithelial cells
DNMT	DNA methyltransferase
DNMTi	DNMT inhibitor
HDAC	Histone deacetylase
HDACi	HDAC inhibitor
VEGF	vascular endothelial growth factor
OC	Ovarian cancer
AZA	5-azacytidine (a DNMTi)
MS, MS275	Entinostat (an HDACi)
ITF, ITF2357	Givinostat (an HDACi)
CTA	Cancer testis antigen
NK cell	Natural killer cell
DC	Dendritic cell
MDSC	Myeloid derived suppressor cell

List of Tables

List of Figures

A) Schematic of AZA *in vitro* treatment. Media was changed and replaced with fresh 500nM AZA on the days indicated with arrows. **B and C)** Western blots of DNMT1 levels at day 3 and 10in ID8-VEGF-defensin cells and the quantification (n=3). **D and E)**

Chapter 1: Introduction

Epigenetics in Cancer

Epigenetics is the study of heritable changes to gene expression that are not caused by changes in the DNA sequence itself (1-4). Types of epigenetic modifications include DNA methylation and histone modifications such as methylation and acetylation (1). DNA methylation is found on the cytosine in a CpG dinucleotide, and in normal cells is found primarily in noncoding regions of the genome (3). This is in contrast to the promoter regions of certain genes that contain a density of CpG dinucleotides, or CpG islands, which are usually unmethylated (3). However, transcriptionally silenced genes on the inactivated X chromosome of females are associated with highly methylated CpG islands (3,5). DNA methylation can also occur in gene bodies, where it is associated with gene expression (6). DNA is methylated by one of three DNA methyltransferases: DNMT1, DNMT3a, and DNMT3b (7). DNMT1 is the principal methyltransferase responsible for the maintenance of methylation in replication, during which it targets hemi-methylated DNA at replication foci via interactions with the protein UHRF1 (8,9). While DNMT1 can add *de novo* methylation in cancer cells (10), DNMT3a and 3b are thought to be primarily responsible for *de novo* methylation in normal cells (7,11), and are perhaps influenced by sequences adjacent to the target CpG sites (12).

Histone modifications change the packaging of the DNA, which can be in euchromatin, where nucleosomes are less tightly packaged, or in the more condensed heterochromatin, altering its accessibility to transcription factors and therefore gene expression (13,14). Histone modifications are added by histone acetyl transferases (HATs) and histone methyltransferases, while they are removed by histone deacetylases (HDACs) and histone demethylases (15). There are 18 identified HDACs that are classified by cellular localization and cofactor requirements (16). Class I HDACs are located in the nucleus, and include HDAC1, 2, 3, and 8. HDAC1 and 2 are especially critical in terms of histone deacetylation and in repressive complexes, discussed further

below (16,17). Class IIa HDACs (4, 5, 7, and 9) can be either nuclear or cytoplasmic, while Class IIb HDACs (6 and 10) are found in the cytoplasm, along with the single Class III HDAC, HDAC11.   Acetyl groups on histones neutralize the charge on the protein, removing steric hindrance and allowing transcription factor localization (15). Therefore, histone hypoacetylation at the promoter region of genes caused by HDACs is associated with tighter chromatin structure and the silencing of genes (18,19).

In cancer, epigenetic modifications can be deregulated and aberrantly changed. For example, promoter hypermethylation is one of the most well-studied epigenetic abnormalities in cancer (3,20). In cancer cells, increased methylation at promoters, where DNA transcription begins, is associated with the silencing of genes, which can include tumor suppressor genes such as *BRCA1/2*, *TP53,* and *CDKN2A* (p16) (21). In contrast, gene body methylation is generally decreased in cancer (22). Changes in histone acetylation are also associated with cancer, namely, decreases in the active mark of histone acetylation at gene promoter regions where the DNA has been hypermethylated (23). Furthermore, histone deacetylases are often overexpressed in cancers (18).

Epigenetic Inhibitors

Because of the epigenetic changes that occur in cancer cells, both DNA methyltransferases and histone deacetylases have been targeted for cancer therapy. Demethylating agents, such as 5-azacytidine or decitabine, re-express aberrantly silenced genes in cancer cells by incorporating into the DNA as cytidine analogs, leading to the degradation of DNA methyltransferases and a decrease in DNA methylation (24). Specifically, 5-azacytidine (AZA) is transported into cells and converted to decitabine by ribonucleotide reductase (25). Decitabine is incorporated into DNA, as is 10-20% of AZA, while the remaining intracellular AZA is incorporated into RNA (26). There, it has

effects on ribosome biogenesis and protein synthesis (27). Because both agents are incorporated into replicating DNA, cells need to be in S phase for effective demethylation (28). Once incorporated as a cytosine, the decitabine binds covalently to the DNMTs, which leads to their degradation (29,30). Because of the subsequent lack of DNMTs, methylation is passively lost as the cell divides. Both AZA and decitabine have been FDA approved for treatment of myelodysplastic syndromes and chronic myelomonocytic leukemia (31). A newer demethylating agent, guadecitabine or SGI-110, is a novel dinucleotide consisting of decitabine and deoxyguanosine, which renders the molecule less susceptible to degradation by cytidine deaminase. This can improve the stability and half life of the drug (16,32).

Histone deacetylase inhibitors (HDACi) increase gene expression by inducing histone hyperacetylation and chromatin remodeling (33). They function by chelating zinc away from the active site of the deacetylase (34). Different types of HDACi, including benzamides, hydroxamic acids, cyclic peptides and aliphatic fatty acids, target individual HDACs with different specificities (16,34). Entinostat, a benzamide, selectively inhibits certain Class I HDACs, with nanomolar level K_i values for nuclear HDACs 1 and 3 (34). In a phase II trial of ER+ breast cancer, the addition of entinostat to exemestane significantly increased progression free survival and overall survival (35), and it was combined with AZA in a Phase I/II trial in patients with non small cell lung cancer, with objective responses observed in individual patients (discussed below) (36). A less well known HDACi is Givinostat, a hydroxamic acid that targets class I HDACs 1, 2 and 3 as well as the cytoplasmic Class IIb HDAC 6. Givinostat has been tested in a phase II clinical trial with patients with multiple myeloma (37), where it was tolerable and provided modest benefit, but not yet in solid tumors. Other HDACIs are already FDA approved for heme malignancies, including the hydroaxamic acids panobinostat, belinostat, and vorinostat, and the cyclic peptide romidepsin (16).

4

Combination Epigenetic Therapy

DNA methylation and histone deacetylation are linked events in their control of gene expression. Each DNMT has been shown to bind HDAC1 and 2 (38-42). Furthermore, DNA methylation can attract methylcytosine-binding proteins MBD1, MBD2, MBD4, MeCP1, and MeCP2 (43,44), which mediate transcriptional repression and heterochromatin formation via recruitment of a corepressive complex that includes HDAC1 and HDAC2 (43,45,46). Specifically, MBD2 or 3 interacts with this nucleosome remodeling and deacetylase complex (NuRD) (47). HDACs 1 and 2 are a dimer in the NuRD complex and facilitate its deacetylase activities (17) Furthermore, they interact in the NuRD complex with CHD4, an ATPase in the SWI/SNF family that compacts nucleosome structure (48). Therefore, there is a direct link between DNA methylation, HDACs, and chromatin remodeling through the NuRD complex. Another repressive complex is the nuclear receptor corepressor (NCoR) and silencing mediator for retinoid and thyroid receptor (SMRT) complex (49). This complex, which includes HDACs 3, 4, 5, and 7, is linked to DNA methylation through the interaction with MeCP2, a methyl-cytosine binding protein, which is required for the transcriptional repressive activity of the complex (46). Because DNA methylation and histone deacetylation are linked by repressive complexes that reconfigure chromatin, targeting both DNMTs and HDACs is a promising strategy for cancer therapy.

Because of the interactions of the epigenetic changes that occur in tumor cells, progress has been made in the therapeutic strategy of targeting multiple epigenetic mechanisms (23,50). In preclinical work in cell culture and animal studies, low doses of both a demethylating agent (DNMTi) and a histone deacetylase inhibitor (HDACi) have been shown to synergistically re-express silenced genes and lead to greater anti-tumorigenic effects (16). For example, in colorectal cancer cells, demethylating agents given prior to HDACIs worked synergistically to re-express hypermethylated genes (51),

likely because hypermethylation is associated with deacetylated histones (52,53). Similar results were found in human lung cancer cells, where cell death was induced by the combination of an HDACi and the demethylating agent decitabine, perhaps by allowing increased transcription of pro-apoptotic genes (54).

As in cell culture, many animal model studies have shown that the combination of a demethylating agent with an HDACi can increase the re-expression of silenced genes and reduce tumor burden more than either single epigenetic drug. In one such study, the combination of the HDACi belinostat and decitabine increased the sensitivity of xenografts ovarian tumors to cisplatin, along with increasing the *in vivo* expression of genes implicated in cisplatin sensitivity (55). In another xenograft model of ovarian cancer, the combination of decitabine and the HDACi vorinostat decreased the growth of the cancer cell line *in vitro* and *in vivo*, while inducing apoptosis, G2-M arrest, autophagy, and the expression of tumor suppressor genes (56). Synergy in tumor reduction was also seen in a hepatocellular carcinoma xenograft model treated with decitabine and vorinostat (57) and in the Calu-6 lung cancer line treated with 5-azacytidine and entinostat (58) or guadecitabine and entinostat (59). With AZA and entinostat, pro-apoptotic genes were found to be upregulated in the lung cancer model by the combination therapy (58). Finally, in a genetically engineered mouse model of medulloblastoma and rhabdomyosarcoma, the combination of decitabine and the HDACi valproic acid prevented tumor incidence, while reducing DNMT1 activity and inducing hyper acetylation. This therapy was not effective in later stage tumors in this model (60).

There are several clinical trials that have tested combination epigenetic therapy in patients. Specifically, the combination of a demethylating agent and a histone deacetylase inhibitor has been shown to be effective in individual patients with non-small cell lung cancer (36). Stable disease was observed in patients with mixed tumors treated with 5-azacytidine and valproic acid given concurrently (61) and with decitabine

and vorinostat given sequentially (62), and in patients with non small cell lung cancer who were treated with decitabine and valproic acid sequentially (63). Trials are ongoing with AZA and entinostat in advanced HER2 negative breast cancer and colorectal cancer (16,23).

In patients that received the combination epigenetic therapy in the NSCLC trial (36), 6 patients had progressive disease and continued on to a trial using α-PD-1 and PD-L1 checkpoint blockade. Of those six patients, five received clinical benefit from the immunotherapy, which was greater than the rate of response in the general patient population (64). This suggested that there may be a sensitization effect of combination epigenetic therapy for immune checkpoint blockade.

Immune Checkpoint Blockade

Immune checkpoint blockade is therapy that involves targeting receptors on T cells or their ligands that regulate the activation of the immune cells (65). One of the most well studied immune checkpoints is the inhibitory PD-1/PD-L1 interaction (66-69). PD-1 is induced on T cells after they have been activated (70), and PD-L1 upregulation by tumor cells is a mechanism of tumor immune evasion (69). In situations where T cells are chronically exposed to an antigen, like in the case of cancer, PD-1 can be highly expressed in antigen specific T cells, which can lead to an exhausted or anergic state that can be relieved by inhibiting PD-1 (71). While PD-1 is mostly studied on T cells, it can also be found on natural killer cells and B cells (72,73). Another well studied immune checkpoint is the CD28/CTLA-4 interaction, as the CTLA-4 molecule blocks the co-stimulatory action of CD28 on T cells by binding to its ligands CD80 and CD86 (74). Finally, there are several more novel checkpoints, including LAG-3, natural killer inhibitory receptors, B7-H3, and TIM-3, all of which may be targeted, perhaps in combination with other checkpoint inhibitors (75).

In patients, targeting of the inhibitory PD-1/PD-L1 interaction has been accomplished with α-PD-1 or α-PD-L1 antibodies, and has been successful in treating advanced, metastatic cancers, especially melanoma, renal cell carcinoma, and non-small cell lung cancer (75-81). There may be a link between the tumor expression of PD-L1 and the rate of response to α-PD-1 or α-PD-L1 therapy (75). Anti-PD-1 therapy has been FDA approved in melanoma and non-small cell lung cancer (75), and one exciting aspect of the success of immunotherapy is that it can produce durable responses (82).

While there are exciting advances and successes with immune checkpoint blockade, a majority of patients still do not respond (75,83). Recently, combination therapy has been used to improve outcomes of immune checkpoint blockade. In melanoma, combining α-PD-1 with another checkpoint inhibitor, α-CTLA-4, has been successful (84,85). There have also been studies of combination with conventional therapies; for example, in renal cell carcinoma, the addition of a multi-receptor tyrosine kinase inhibitor, sunitinib or pazopanib, to α-PD-1 therapy improved the response rate to 40-50% (83). Conventional therapy can have immunologic effects that make it a potentially good combination with immune therapy; for instance, in melanoma, the BRAF inhibitor vemurafenib increases the expression of tumor antigens and antigen presentation molecules (86).

Combining Epigenetic and Immune Therapies

After making the previous observation that a small number of patients who received immune checkpoint blockade therapy after combination epigenetic therapy had robust and durable tumor responses (64), our lab and others studied how epigenetic therapy may prime tumors for immune therapy. *In vitro* studies have shown that epigenetic agents can have immunogenic effects. For example, cytotoxic cell killing can

release tumor antigens (83). In a more specific way, epigenetic therapy can cause the

upregulation of immune genes in tumor cells (87). One well established form of this is

the upregulation of cancer testis antigens, which are genes that are expressed in

development, but normally methylated and silenced in somatic cells, although they can

lose the methylation and be expressed in cancer cells (88-90). Cancer testis antigens

that can be re-expressed with DNA demethylating agents include MAGE-A1 and NY-

ESO-1 (90). In ovarian cancer, cancer testis antigen expression was associated with

promoter DNA hypomethylation (91), and NY-ESO-1 and MAGE-A were shown to be

able to be re-expressed in ovarian cancer xenografts by SGI-110, a DNMTi, which then

made the xenografts more sensitive to NY-ESO-1 specific CD8$^+$ T cells (92). This

preclinical data culminated in a successful phase 1 clinical trial combining decitabine, an

NY-ESO-1 vaccine and doxorubicin chemotherapy in patients with epithelial ovarian

cancer where there was stable disease or partial clinical response in 6/10 patients (93).

Our lab also found that CTAs were significantly upregulated by AZA in a majority of 77

breast, colorectal, and ovarian cancer cell lines (87).

In addition to cancer testis antigens, other forms of tumor antigens can be re-

expressed by epigenetic therapy. For example, in a mesothelioma xenograft model,

combination treatment with DAC and valproic acid attracted tumor antigen specific CD8$^+$

T cells to the tumor and decreased tumor growth (94). The re-expression of the death

receptor Fas in tumor cells after decitabine and vorinostat is another example of how

epigenetic gene re-expression helped sensitize tumors to immune therapy, as those

tumors were more sensitive to tumor specific cytotoxic lymphocyte adoptive

immunotherapy and metastatic burden was reduced (95). Other types of immune genes

upregulated by epigenetic therapy in the published literature include antigen processing

and presentation pathway genes, interferon signaling, and chemokines and cytokines

(87). This set of pathways included genes encoding proteins involved in the proteasome

as well as MHC class proteins, and was concordant with observations made previously in cancer cells treated with decitabine (90). In ovarian cancer, an upregulation of chemokines was observed by other groups also using decitabine (96,97). Because not all of these genes are classically regulated by methylation, the upregulation of these immune pathways may be downstream of another mechanism.

Interferons are a type of cytokine that have anti-viral, anti-proliferative, and immunomodulatory downstream effects (98). The name interferon comes from their ability to "interfere" with viral infections. There are two main classes of interferon signaling, Type I includes IFN-α, IFN-β, IFN-ε, IFN-κ and IFN-ω, while Type II is only IFN-gamma (99,100). Both signal through interferons receptors made up of 2 subunits: IFNAR1 and 2 for type I interferons, and IFNGR1 and 2 for the type II interferon signaling (98). Both then signal through the classical JAK/STAT pathway (101,102) and induce the expression of hundreds of genes, with some of those being differentially regulated by the distinct interferons (103). Type I interferon signaling has numerous downstream effects that can contribute to anti-tumor immunity, including stimulating dendritic cells to present antigen to cytotoxic lymphocytes (104-106), providing the "third signal" needed for the expansion of activated CD8^{+} T cells (107-109), and increasing the viability of the activated T cells (110). Likewise, interferon gamma binding to its receptor culminates in immune cell activation (111), and signaling in tumor cells can directly inhibit tumor growth (111-113). However, exposure of tumor cells to interferon gamma can induce the adaptive resistance mechanism of expressing PD-L1 (114,115).

Interferon signaling in tumors was first shown to be upregulated by demethylating agents by Karpf et al (116) in colon cancer cells. There, decitabine treatment increased STAT1, 2, and 3 signaling and activation through interferon-α and sensitized the cells to interferon-α treatment. In ovarian cancer patients, it was observed that cytokines and JAK/STAT pathway genes were upregulated in patients treated with decitabine and

carboplatin (117). In our work, interferon signaling was found to be enriched by AZA treatment of 77 different epithelial cancer cell lines (87). Together with other enriched immune related genes, like the CTAs, chemokines, cytokines and antigen presentation and processing genes described above, a 314 gene panel was derived to categorize tumors as "high" or "low" for the AZA induced immune genes, or AIM (87).

Recently, the interferon pathway was shown to be upregulated in tumor cells by the demethylation and re-expression of endogenous retroviruses by AZA treatment (118,119). Endogenous retroviruses make up about 8% of the human genome (120), and are usually silenced by methylation (121), though they can be demethylated and expressed in some tumors (122). DNA methyltransferase inhibitor (DNMTi) treatment of ovarian cancer cells upregulates ERVS, leading to dsRNA which triggers the cytosolic RNA sensors TLR3 and MDA5 and creates a downstream signaling pathway through type I interferon and JAK/STAT (118). Similar results were shown in colon cancer cells, with the addition of showing that the interferon response was necessary for the inhibition of colon cancer stem cells by DNMTIs (119). The downstream effects of interferon signaling in the tumor cells are apoptosis and the induction of other interferon stimulated genes such as those involved in cytokine production, as well as antigen processing and presentation. One gene that is crucial to the interferon response, *IRF7*, is in fact controlled by methylation of its promoter, and its knockdown significantly reduces the interferon response induced by DNMTi in ovarian and colon cancer cells (118,119). A subgroup of interferon stimulated genes that were upregulated by AZA in cancer cell lines, the viral defense signature, was able to sort ovarian carcinomas into baseline high and low ISG expression, which correlated with ERV expression. Excitingly, AZA treatment sensitized the B16 murine melanoma cells to α-CTLA-4 *in vivo* (118), with the combination therapy significantly reducing the tumor burden compared to either therapy

11

alone. This synergy could be extremely relevant to patients, as responses to anti-CTLA-4 in melanoma patients correlated with high baseline levels of viral defense genes (118).

The interferon response in tumor cells has been shown to be important for the tumor response to therapy. The downregulation of the interferon alpha receptor 1 (IFNAR1) in colon cancer cells has been shown to enable an immune privileged niche which promotes the growth of colorectal carcinoma cells, while the stabilization of IFNAR1 improved cytotoxic lymphocyte survival and the efficacy of α-PD-1 therapy (123). This supports the rational that upregulating IFNAR1 is beneficial to cancer therapies (123). Likewise, the loss of interferon gamma pathway genes in tumor cells can be a mechanism for resistance to α-CTLA-4 (124). Because α-CTLA-4 therapy stimulates interferon-γ production by T cells, one downstream effect is the binding of interferon gamma to its receptor on tumor cells, which can lead to the inhibition of tumor cell growth through JAK1 and 2 and STAT1 signaling (124). On the other hand, prolonged tumor interferon signaling itself has been shown to induce resistance to immune checkpoint blockade over time (125). Specifically, interferon signaling can upregulate interferon stimulated genes which include ligands for multiple T cell inhibitory receptors (125). This will be an important subject for future studies, and the timing and duration of an immune response in tumor cells may be of critical importance.

In addition to affecting the immunogenicity of tumor cells, epigenetic therapy is known to affect host immune cells as well. The HDACIs vorinostat and panobinostat were found to require an intact immune system for anti-tumor efficacy in syngeneic models of colon cancer and lymphoma (126). Interestingly, interferon- γ receptor signaling in the tumor cells was important for the anti-tumorigenic effect. The authors found that in this case, B cells, but not natural killer or CD8$^+$ cells were important for the response, and concluded that combinations of HDACi with immunotherapy could be appropriate because of their immunostimulatory effects (126). HDACIs were found to

also affect T cells by enhancing effector T cell survival and decreasing T_{regs} in the B16 mouse melanoma model, and by increasing the stimulatory molecules OX-40 and CD25 on T cells (127). HDACIs have also been shown to reduce myeloid derived suppressor cells in the tumor microenvironment (128,129). Finally, low doses of decitabine have been shown to enhance NK cell killing of AML cells (130).

Epigenetic and Immunotherapy in Ovarian Cancer

Based on the background of evidence that epigenetic agents could enhance the immune response to tumors, we decided to look into the effect of combination epigenetic therapy in ovarian cancer. The upregulation of immune gene sets by AZA was highest in human ovarian cancer cell lines compared to breast, colon, or lung cancer cell lines (87). Furthermore, anti-tumorigenic effects have been observed with different epigenetic therapies and immune therapies in other mouse models of ovarian cancer. Decitabine was able to increase the activation of CD8$^+$ and natural killer (NK) cells in the ascites fluid of tumor bearing mice, and it also sensitized ovarian tumors to α-CTLA-4 therapy (96). Combining an inhibitor of another epigenetic repressive enzyme, the histone methyltransferase EZH2, with decitabine increased the expression of chemokines in the tumor, and sensitized the tumor to α-PD-L1 (97). Because of the ability of HDACi to enhance the effects of a demethylating agent and its potential to influence the immune microenvironment of the tumor, as described above, we hypothesized that combining the demethylating agent 5-azacytidine with and HDACi could sensitize tumors to immune checkpoint blockade.

In this study, we used syngeneic as well as immunodeficient mouse models to identify the actions of the epigenetic agents, alone or in combination, on the tumor cells themselves, and then determined whether an immune system is required for their effects. First, we have characterized the tumorigenicity and response to AZA of four

related syngeneic ovarian cancer cell lines, and determined the best methods for measuring their tumor burden, as described in Chapter 2. Next, in Chapter 3, using the cell line that formed tumors in mice the most consistently and quickly, we have shown that AZA treatment also decreases tumor burden, extends survival, and increases the activation of tumor killing immune cell subsets, in part through type I interferon signaling. When both AZA and an HDACi are administered, combination therapy is significantly better than either drug alone in terms of tumor burden, survival, and immune cell activation. Furthermore, the benefit in terms of tumor reduction is absent when the cells are injected into NSG mice instead of the immunocompetent model, suggesting that the immune system is important for the effect of the AZA and HDACi combination treatment. Most importantly, the combination of AZA and an HDACi sensitized these murine ovarian tumors to α-PD-1 therapy, which may indicate that combination epigenetic therapy could benefit patients who may not respond to immune checkpoint blockade.

Chapter 2: The Characterization of Murine Ovarian Cancer Cell Lines and Development of a Mouse Model of Ovarian Cancer to Evaluate Tumor Response

Summary

In order to study tumor development in the context of a complete immune system, it is necessary to have a functional syngeneic model, meaning that the tumors are derived from the same genetic background of the host. In 2000, K. Roby developed a series of mouse ovarian surface epithelial cell lines and cultured them *in vitro* until they spontaneously immortalized (131). These cell lines were then transplanted into mice to form tumors and have formed the foundation for numerous mouse models of ovarian cancer. Particularly, the ID8 clone has advanced studies of tumor immunosuppression. Since their development, the cell lines have been engineered to express GFP, luciferase, and VEGF and defensin, in order to better monitor tumor burden, accelerate tumor growth, and to study the effects of those molecules on ovarian cancer (132-134). Here, we describe the phenotypic differences between cell lines from the original Roby paper (Roby-ID8-nonluc), one with luciferase added (Roby-ID8-luc2), one derived from a tumor formed by Roby cells (MOSEC) and one expressing GFP, luciferase, VEGF, and defensin (ID8-VEGF-defensin). These cell lines have varying abilities to form tumors in mice. In the case of the Roby-ID8-nonluc cells, passaging the cells *in vivo* increased the consistency of ascites formation and accelerated development time. All three cell lines responded to the demethylating agent 5-azacytidine as expected, with a decrease in cell numbers compared to untreated cells and a decrease in DNA methyltransferase 1 levels. Finally, we assessed which parameters would be best used to determine the tumor burden of the mice. Luciferase activity was increased in AZA treated cells, and did not correlate well with survival, ascites or weight gain. On the other hand, ascites did correlate significantly with weight gain, and decreased ascites burden correlated with longer survival. Therefore, we have established the tumorigenicity of a syngeneic ovarian cancer model, characterized its response to AZA *in vitro*, and subsequently determined the best ways of measuring the tumor burden of the mice.

Introduction

Ovarian cancer is the most lethal gynecological malignancy in the United States (135), and there is a need for new therapies; therefore, having models to study ovarian cancer is of critical importance. Thus far, the absence of reliable mouse models has been a hindrance to ovarian cancer research (136). One reason for this is that the understanding of the origin of ovarian cancer has recently advanced with the discovery that high grade serous ovarian carcinoma may arise from the fallopian tube (137,138). However, there is also recent data that the ovary itself plays an important role in the pathogenesis of ovarian cancer in mouse models (139,140) and in patients (141). There are transgenic models that mimic the development of cancer in the fallopian tube (142,143). However, the ID8 model (described in detail below) is the only transplantable syngeneic murine model of ovarian cancer routinely available, and it has been used in over 100 publications (144). In our study, we treated the tumor cells both *in vitro* and *in vivo*, so it was necessary to have a model that could be manipulated outside of the mouse. Also, in testing multiple drugs in combination, the size of the experiments could have been prohibitively large using a transgenic model, because often the cohorts of mice that develop tumor at the same time are smaller.

Besides syngeneic and transgenic models, xenograft models have been used in ovarian cancer research (145). However, those were ruled out for our study because we wanted to research how ovarian tumors interact with the immune system and how this affects the tumor response to therapy. Immune evasion is an important step in the development of most cancers (146). In ovarian cancer patients, it is known that the presence of intratumoral T cells and immune signaling in the tumor correlate with a better prognosis and improved overall survival (147). Furthermore, immune signaling was found to be enriched at baseline in a subset of patients with longer progression free survival in a phase II clinical trial (117). Because of the importance of the immune

system in the progression of ovarian cancer and in determining the response to therapies, it was critical to use a model of ovarian cancer in which the tumor develops in the presence of an intact immune system.

In order to address the need for immunocompetent models of ovarian cancer, cell lines were developed from the ovarian surface epithelium of C57Bl/6 mice (131). After cells were trypsinized from the ovaries, they transformed after passaging *in vitro*. Later passage mouse ovarian surface epithelial cells (MOSECs) form small tumor nodules and cause hemorrhagic ascites fluid when injected intraperitoneally into immune competent C57Bl/6 mice. Ten clones were obtained from late passage MOSECs, which caused the accumulation of ascites fluid between 22-48 days after the injection of 5×10^{6} cells (131). One specific clone, ID8, has been used extensively by ovarian cancer researchers. We have received two versions of the ID8 clone from Katherine Roby, one expressing luciferase and one the non-luciferase control cell line. We have referred to those lines as Roby-ID8-luc2 and Roby-ID8-nonluc (Figure 2.1A). Our lab was also gifted MOSECs without a specified clone number that were derived from a tumor by Chien-Fu Hung of Johns Hopkins University Department of Pathology (Figure 2.1A). The ID8 line has been changed substantially, as outlined in Figure 2.1A, to generate a more aggressive line that is more representative of ovarian cancer, and the last cell line that we use in this study is a derivative of that line referred to as the ID8-VEGF-Defensin cells, which also express GFP and luciferase. These cells were developed over several years and labs. First, in order to study the effects of VEGF on tumorigenesis, ID8 cells were generated that expressed vascular endothelial growth factor (the murine VEGF164 isoform) and green fluorescent protein (GFP) (132). This decreased the time to tumor formation considerably (132,148). Furthermore, beta-defensin-29 was transduced into the cells (133), which increased tumor growth and vascularization, followed by luciferase

(134). In these models, ascites development is often a measure of tumor load (133,148-154), as well as luciferase activity as detected by bioluminescence imaging (134,149).

In our study, we have characterized four of the cell lines derived from the mouse ovarian surface epithelial cell lines first established by Roby et al. The lines are Roby-ID8-luc2, Roby-ID8-nonluc, MOSEC, and ID8-VEGF-defensin (Figure 2.1A). For each line, we have determined its tumorigenicity in mice, and in the case of the Roby-ID8-nonluc the tumorigenicity has been improved with repeated passages. The cell lines responded to the demethylating agent 5-azacytidine as expected, with a loss of cell viability and a decrease in the protein levels of DNMT1. We have shown that measuring the weight gain and ascites burden of the mice, and not the luminescence of the tumor, is the best way to measure the tumor burden in this model, as the ascites volume most closely correlates with the survival of the mice, and the luciferase activity in the cells is increased as the viral promoter driving the expression can be demethylated following treatment with AZA. In conclusion, we have successfully determined which of several models of ovarian cancer that can be transplanted into immune competent mice would be best to use to study tumor response to therapy as well as the interaction with the immune system in the tumor microenvironment.

Methods

Cell lines and treatment

MOSE ID8-Defb29/Vegf-a (ID8-VEGF-Defensin) cells and Mouse ovarian surface epithelial cells (MOSECs) were kindly provided by Dr. Chien-Fu Hung, Johns Hopkins Pathology. Roby-ID8-luc2 and Roby ID8-nonluc were kindly provided by Dr. Katherine Roby. All four cells lines were grown in RPMI medium, with 10% FBS and gentamicin (5mg/mL), split every 3-4 days, and treated with AZA (500nM). The AZA (Sigma)

treatment schedule consisted of the media being changed and refreshed with 500nM

AZA on days 1, 2, 3, 6, 7, 8, and 9. Cells were split on days 3 and 6.

Mouse Experiments

Cells (0.5, 2.5 or 5 million) were injected intraperitoneally in 6-8 week old C57Bl/6 mice.

Tumor burden was assessed via measurement of body weight and amount of ascites

drained from the mice at the point when they gained 20-30% of their body weight. Mice

were cared for in accordance with the policies of the JHU ACUC.

Ascites Serial Transplantation

Ascites were drained from individual mice and incubated in ACK buffer (Thermo Fisher)

to lyse red blood cells for 10 minutes, then washed. Tumor cells were counted using a

hemacytometer, and injected i.p. back into non-tumor bearing secondary or tertiary mice.

Cell proliferation assays

Cells were plated in triplicate, then treated with AZA the following day for up to 10 days

of treatment. Cells were trypsinized and counted at days 3 and 7 and 10, and the same

number of Mock or AZA treated cells were replated. Trypan blue was used to determine

viability.

Western Blots

Protein extracts were quantified and immunoblotted using the 4%–20% Mini-PROTEAN

TGX gel system (Bio-Rad) and PVDF membranes (Millipore). β-actin or GAPDH was

used as a loading control. Antibodies used were as follows: polyclonal rabbit anti-

DNMT1 (Sigma , 1:1000), mouse anti-β-Actin (Sigma, 1:10,000), and polyclonal rabbit

anti-GAPDH (Trevigen, 1:10,000).

Luminescence Assay

Luminesence was measured using the Dual Luciferase Reporter Assay System

(Promega, E1910). Cells were plated and treated with an A3 or A10 schedule, then

trypsinized. An equal total number of treated or untreated cells were aliquoted for the

assay.

Measuring tumor bioluminescence

D-luciferin (Perkin Elmer, 150mg/kg) was injected into mice bearing luciferase

expressing tumor cells. Eight to twenty minutes after D-luciferin injection, mice were

anesthetized with isoflurane, and the bioluminescence was imaged using the IVIS

Spectrum In Vivo Imager.

Statistical analysis

Data was graphed in GraphPad PRISM 5.0, and significance was determined by a

Mann-Whitney t-test, where *= $p < 0.05$; **=$p < 0.01$; ***<$p < 0.001$. Linear regression

analysis in GraphPad PRISM was used to determine the correlation of the parameters of

tumor burden.

Results

Characterization of the tumor forming capability of murine ovarian cancer cell lines

In order to be able to use the murine ovarian cancer cell lines to assess tumor

response to therapy, it was necessary to determine if and how quickly the different cell

lines developed tumors in immunocompetent mice. Weight gain was measured weekly

as a way to quantify the ascites development. The ID8-VEGF-defensin cells grew the

most quickly in mice, with an injection of 500,000 cells causing 30% weight gain from

baseline in just 3.5 weeks (Figure 2.1B). The MOSEC line grew more slowly: 2.5 million

or 5 million cells injected caused 20-30% weight gain in 4 or 5.5 weeks, respectively;

doubling the number of cells injected decreased the time to ascites development by 1.5

weeks (Figure 2.1B). Both the ID8-VEGF-defensin and the MOSEC cells produced

hemorrhagic ascites which correlated with the amount of weight gained (Figure 2.1C). In

contrast to the other two cells lines, the Roby-ID8-luc2 cell line did not develop ascites.

While the mice did gain weight over 18 weeks (Figure 2.1B), there was no swelling of the abdomen, and when the mice were euthanized and dissected, there was no ascites fluid or visible tumor nodules (data not shown).

Because it would be beneficial to have Roby-ID8 cells that could form tumors in immunocompetent mice, we grew the Roby-ID8-luc2 cells that previously did not form tumors for 43 passages in culture. Furthermore, hypothesizing that the luciferase could be having an immunogenic effect that caused the tumor to be rejected by the host immune system, we also tested early and late passages of the Roby-ID8 cell line that does not express luciferase (Roby-ID8-nonluc). The results, found in Table 3.1, showed that the Roby-ID8-luc2 cells that had been passaged still did not develop any ascites, and the mice were euthanized at 11.5 weeks. However, 1/3 of the Roby-ID8-nonluc early passage, and 2/3 of the Roby-ID8-nonluc late passage cell lines did develop ascites, at 11 or 12 weeks. This ascites fluid was transplanted into secondary non-tumor bearing mice, and 2/3 of those mice developed ascites at a faster rate than the primary mice (4 weeks). When cells from these ascites were transplanted into tertiary mice, 2/2 mice developed ascites. In conclusion, we were able to develop Roby-ID8-nonluc cells that could develop ascites more quickly and consistently than the Roby-ID8-luc2 cell line.

Characterization of the in vitro sensitivity of the cell lines to AZA

The demethylating agent 5-azacytidine (AZA) is known to have antitumor effects on cells *in vitro*, such as the induction of apoptosis and cell cycle arrest (118,155-157). Therefore, we tested the sensitivity of these cell lines to AZA, with doses from 50 to 500nM. AZA was given in a 10 day regimen (Figure 2.2A). At day 3 in the ID8-VEGF-defensin cells, there is a significant dose dependent decrease in DNMT1, with the significant decrease at 500nM being sustained at day 10 of treatment (Figure 2.2B, C). In the MOSEC and Roby-ID8-luc2 cell lines, a reduction in DNMT1 was observed at Day

1, especially with 500nM AZA. At days 3 and 10, the dose dependent decrease is still observed (Figure 2.2D, E, F, G). In addition to the expected decrease in DNMT1 protein levels, the number of live cells decreased with AZA. After only 2 or 3 days of 500nM AZA, there was a decrease in the number of ID8-VEGF-Defensin, MOSEC, and Roby-ID8-luc2 cells, which was sustained over the 10 day treatment window (Figure 2.2H-J). In summary, these cell lines respond as expected to AZA in terms of the degradation of DNMT1, and they are all sensitive to the relatively low doses of the drug.

Because we will be measuring the effect of AZA on the cells in mice in order to understand how the tumors respond to the drug in the presence of an immune system, it was important to determine what the best method is for measuring tumor burden *in vivo*. Unlike a xenograft model, these cells are injected i.p. and do not form a measurable flank tumor. Two of the cell lines, ID8-VEGF-Defensin and Roby-ID8-luc2 express luciferase, which can be utilized to measure tumor burden by giving the mice an injection of luciferin and then measuring the resulting bioluminescence. However, in our treatment system, we found that either 3 or 10 days of AZA treatment actually significantly increased the luminescence of cells *in vitro*, compared to the same number of untreated cells (Figure 2.3A). This suggested that luminescence may not be the best way to measure the difference in tumor burden between Mock and epigenetically treated groups. Furthermore, the luminescence of cells (Mock as well as AZA treated) that were then injected into mice, did not correlate well with the amount of weight gained or the volume of ascites fluid (Figure 2.3B, C), which are both established measures of tumor burden in similar ascites producing ovarian cancer models (133,148-154). Most importantly, luminescence did not correspond to survival of the mice (Figure 2.3D). On the other hand, ascites and weight did correlate with each other, as expected, and lower ascites volume correlated with increased survival of the mice (Figure 2.3E, F, G). In conclusion, when measuring the effect of treatment on tumor burden and response *in*

vivo, weight gain and ascites fluid are the best measures in this model, while luminescence does not accurately reflect tumor burden in response to AZA treatment.

Discussion

Out of the first three murine models of ovarian cancer tested for tumorigenicity in C57Bl/6 mice, two (MOSEC and ID8-VEGF-defensin) caused tumor formation and ascites development in mice. The third, Roby ID8-luc2, did not induce ascites production in 18 weeks after cell injection i.p.; however, the non-luciferase expressing versions of this cell line did produce ascites in immune competent mice. One hypothesis for why this is the case is that transgenes, especially those foreign to mouse cells, can be immunogenic and cause rejection of tumor cells by the host (158). Furthermore, of the Roby-ID8-nonluc cells that did produce ascites, the later passage of the cells caused ascites more frequently. This is similar to the earlier observation that the original MOSEC cells only became tumorigenic in mice after ~20 passages *in vitro* (131). As cells grow in culture, they can acquire mutations that provide a growth benefit. Therefore, it was not surprising that we were able to improve tumorigenicity of the Roby ID8 cells by using the non-luciferase expressing, later passage cell line. However, these cells still grew too slowly and the tumor latency was so long that they were impractical to work with and did not represent aggressive late stage ovarian cancer.

In determining the best method of measuring the tumor burden of these models, we established that 5-azacytidine treatment actually increased the activity of luciferase compared to Mock cells. One hypothesis explaining this phenomenon is that AZA could be increasing the expression of the luciferase gene, which is under the control of the viral promoter element in the pMIG-Thy1.1 vector (134). It is possible that a demethylating agent could induce the expression of retrovirally transduced genes (159,160). Therefore, luciferase activity is not the best way to determine the effect of

AZA on the tumor growth of these cell lines that have been retrovirally transduced with luciferase. Because the ascites production of the mice correlated most closely with survival, ascites became the parameter used to determine the tumor burden of the mice, and others use this parameter as well (133,148-154).

While these cell lines are not a perfect model of ovarian cancer in patients, they are a useful model for studying both the tumor and the immune microenvironment. There has been progress made in the understanding that ovarian tumors can arise from the epithelial cells of the fallopian tube, rather than the ovary itself (161), but the MOSEC and ID8 cells are derived from the ovarian surface epithelium. This model also lacks hallmarks of high grade serous ovarian cancer, like the loss of wildtype p53 or dysfunctional homologous repair (144). Recently, cell lines have been derived from the ID8 clone that have been manipulated with CRISPR/Cas9 technology to knock out *Trp53* and Brca2 (144), and these clones may prove to be extremely beneficial for the field because they may provide this useful model with more relevance to patients. However, the models used in this study do have relevance to human disease and benefits for research. Like in the ID8-VEGF-defensin cell line, VEGF can be overexpressed in tumors from ovarian cancer patients, and the cells express the gene at relevant levels (132). Furthermore, the cells are extraordinarily useful in that they can be manipulated outside of the mouse, and then injected into immunocompetent mice and are able to form tumors. The ascites fluid that develops is a critical resource that allows the examination of cells in the tumor microenvironment without sacrificing the mice. In conclusion, these cells provide a clinically relevant model that allows the study of the interactions of the tumor and immune system in a syngeneic setting.

Table 2.1. Increase in the tumorigenicity of the Roby-ID8 cell lines.

		Primary mice: 5,000,000 cells injected	Secondary mice: 5,000,000 cells transplanted	Tertiary mice: 5,000,000 cells transplanted
Cell line	Mouse	Time to ascites	Time to ascites	Time to ascites
Roby ID8 non luc early (p20)	1 2 **3**	none- sac'd at 16 weeks none- sac'd at 16 weeks **11 weeks**	**4 weeks**	**9 weeks**
Roby ID8 non luc late (p38)	1 2 **3**	none- sac'd at 16 weeks **11 weeks** **12 weeks**	**4 weeks** none-sac'd at 24 weeks	**6.5 weeks**
Roby ID8 luc2 late (p43)	1 2 3	none- sac'd at 11.5 weeks none- sac'd at 11.5 weeks none- sac'd at 11.5 weeks		

The Roby-ID8-luc2 and the control cell line lacking luciferase (Roby-ID8-nonluc) were grown in culture for about 40 passages to attempt to increase their capacity to form tumors in mice. 5×10^6 cells of the late passage as well as the Roby-ID8-nonluc early passage were injected i.p. into mice. If ascites developed, tumor cells in the ascites were counted by hemacytometer, and transplanted into secondary mice. The same was done if the secondary mice developed ascites. The time to ascites development was recorded.

<u>Figure 2.1 Related cell lines derived from mouse ovarian surface epithelial cells have different tumorigenicity in mice.</u>

Figure 1
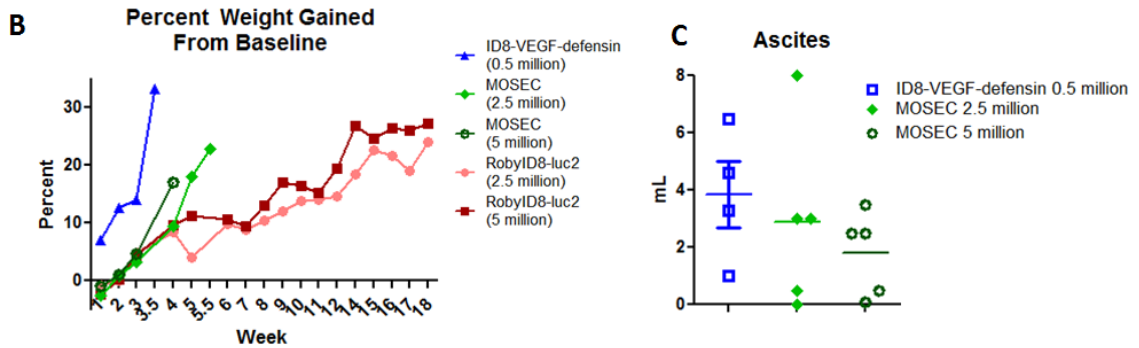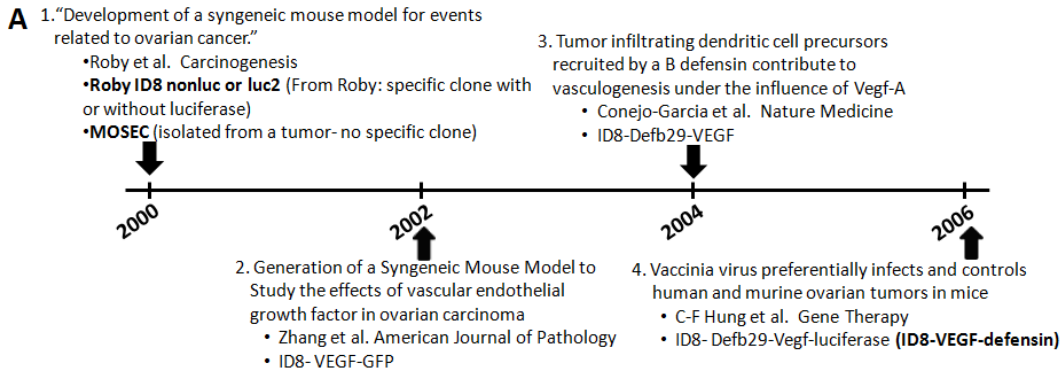
A) A summary of MOSE cell lines that were developed. The bolded cell lines indicate ones used in this manuscript. **B)** The cumulative percentage of weight gained over time. The last point of each line is when ascites was drained. n=4 or 5 mice per group, with one biological replicate. **C)** The amount of ascites drained from the mice.

Figure 2.2 AZA treatment decreases DNMT1 levels and cell number in a dose dependent manner in the ID8-VEGF-defensin, MOSEC, and Roby-ID8-luc2 cells
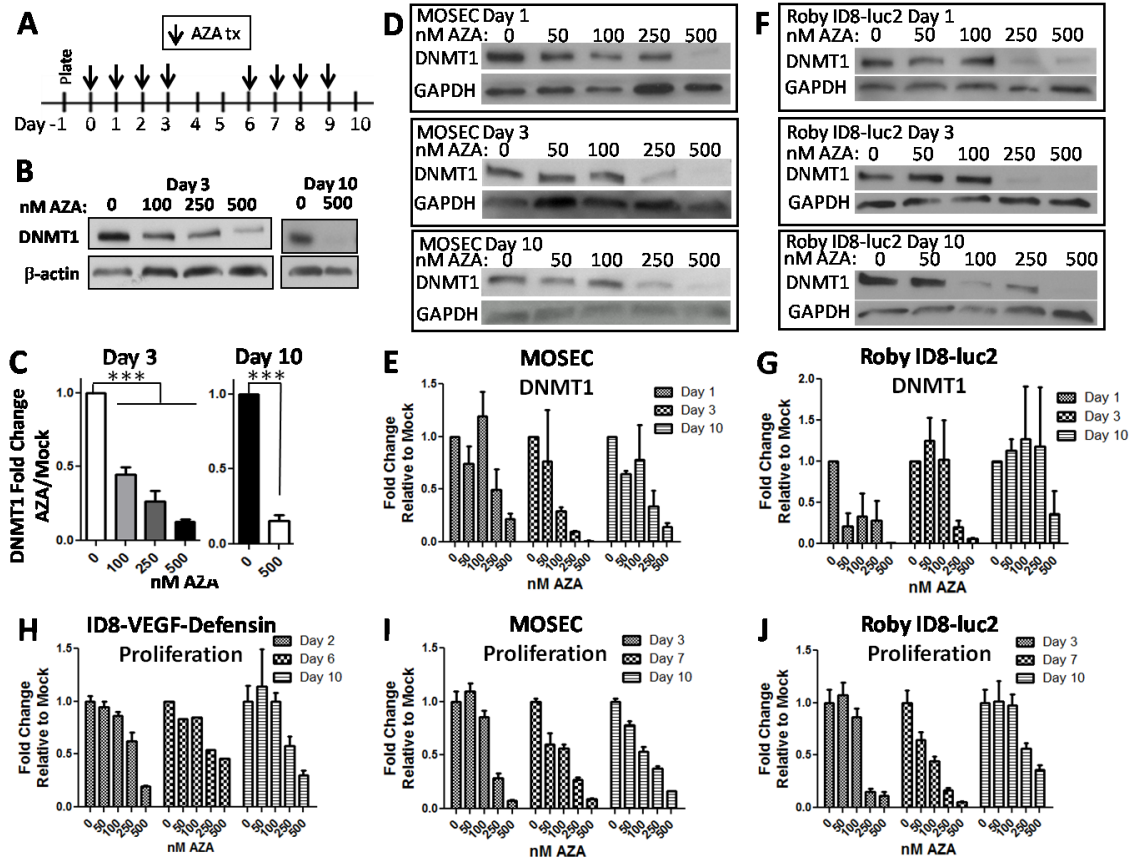
A) Schematic of AZA *in vitro* treatment. Media was changed and replaced with fresh 500nM AZA on the days indicated with arrows. **B and C)** Western blots of DNMT1 levels at day 3 and 10in ID8-VEGF-defensin cells and the quantification (n=3). **D and E)** Western blots of DNMT1 levels in MOSEC cells and the quantification (n=2). **F and G)** Western blots of DNMT1 levels in Roby-ID8-luc2 cells and the quantification (n=2). **H-J)** Number of live cells counted relative to Mock, for AZA treated ID8-VEGF-defensin (n=1), MOSEC (n=2), or Roby-ID8-luc2 (n=2) cell lines.

Figure 2.3: Ascites and weight gain, not luminescence, are the best methods to measure tumor burden in this model.

	r²	Is the slope significantly nonzero? (p value)
Ascites vs. Luminescence	0.003361	0.7609
Weight vs. Luminescence	0.005561	0.6953
Survival vs. Luminescence	0.04635	0.2532
Ascites vs. Weight	0.7569	< 0.0001
Ascites vs. Survival	0.6004	< 0.0001
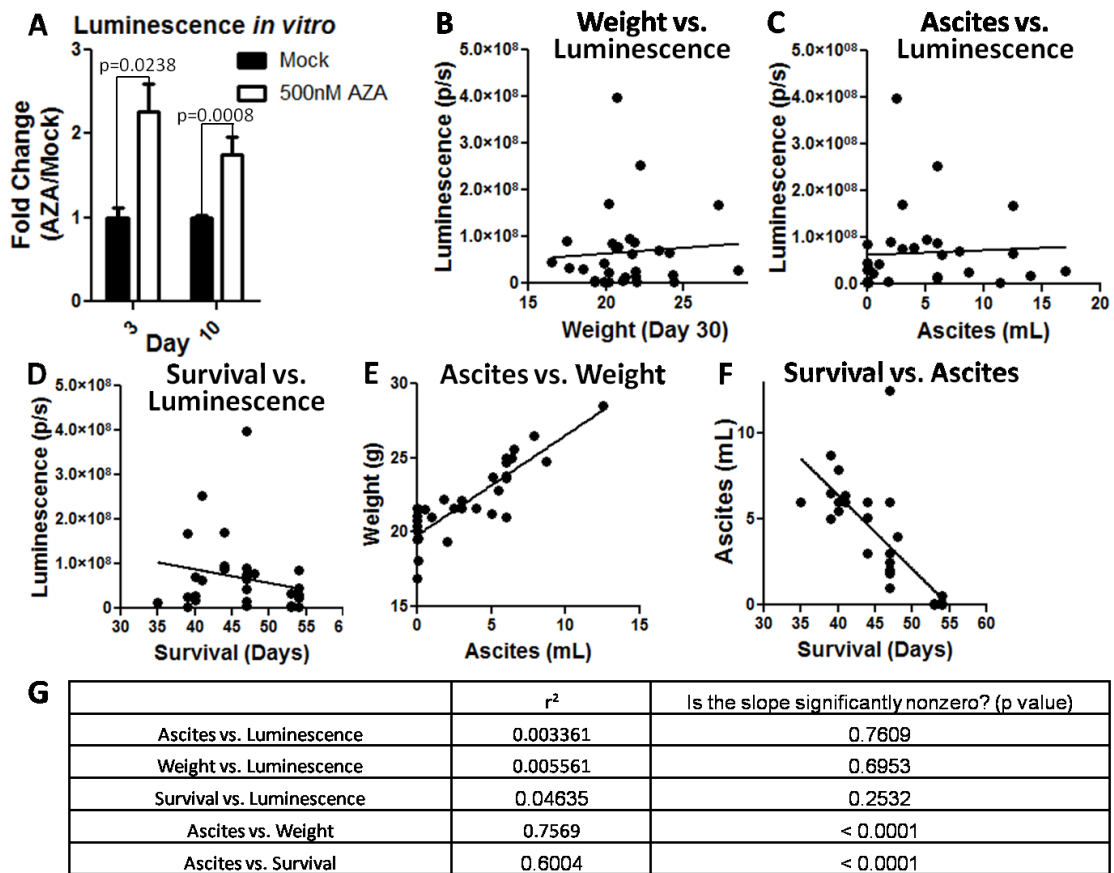
A) Luciferase activity in mock or AZA treated cells. **B-D)** The correlations of different measurements of tumor burden at week 4.5 post tumor cell injection. The luminescence is measured by an IVIS bioluminescence imager, the weight is the number of grams the mice gained in 4.5 weeks, and the ascites burden is the amount of ascites drained by week 4.5. **E)** The r^2 and p values determining the significance of the associations by linear regression.

Chapter 3: Combination epigenetic therapy regulates tumor cells and the immune microenvironment to sensitize ovarian cancer to immune checkpoint therapy.

Summary

Ovarian cancer (OC) is the most lethal of all gynecological cancers and there is an unmet need to develop new therapies. The latest immune therapy approaches to cancer are promising but response of ovarian cancer to these has thus far been disappointing. We now find, in a mouse model of epithelial OC, that clinically relevant doses of DNA methyltransferase (DNMTi) and histone deacetylase (HDACi) inhibitors, improve response to checkpoint inhibitor therapy. The DNMTi, 5-azacytidine, in part via type I interferon signaling, increases numbers of CD45^{+} immune cells, the percentage of active CD8^{+} T and NK cells, and reduces the percentage of macrophages and myeloid derived suppressor cells in the tumor microenvironment. This is accompanied by a reduction in tumor burden by inhibiting proliferation and enhancing apoptosis. Addition of the HDACi to AZA seems to mostly affect immune cells in the tumor microenvironment, specifically increasing T and natural killer cell activation over AZA treatment alone and reducing macrophages. A triple combination of the DNMTi/HDACi plus the immune checkpoint inhibitor, α-PD-1, provides the best anti-tumor effect and prolongs survival.

Introduction

Epithelial ovarian carcinoma is the leading cause of death from gynecological malignancies in the United States (135). Increasing clinical evidence suggests that some ovarian tumors are immunogenic (162,163), yet patient responses to immunotherapy have been disappointing (164). In particular, the response of ovarian cancer to the immune checkpoint inhibitors α-PD-1 or α-PD-L1 has thus far been modest in comparison to the robust responses observed for melanoma, non-small cell lung cancer, and renal cell cancers (76). New treatment strategies are needed to improve the response of ovarian cancers to immune checkpoint inhibitors.

Studies by our group and others have shown that DNA methyltransferase inhibitors (DNMTIs) can upregulate immune signaling in ovarian cancer cells (87,96,97,117,118). This observation led us to question the potential role of epigenetic therapy in the response of ovarian cancer to immunotherapy. The effect of additional epigenetic inhibitors, such as histone deacetylase inhibitors (HDACIs), on the regulation of this tumor cell immune response is not well understood (33). It is known, however, that the use of DNMTIs and HDACIs in combination can often lead to additive or synergistic reactivation of aberrantly silenced genes and cause reductions in tumor burden that are more effective than either epigenetic drug alone (1,16,51,165). Epigenetic therapy using DNMTIs and HDACIs has shown clinical benefit in individual patients with solid tumors (36,166). Important unanswered clinical questions include whether both DNMTIs and HDACIs are needed for an effective epigenetic response, and how the inhibitors act individually and in combination to target the tumor cell and/or the immune microenvironment. Clinical responses have led us to hypothesize that epigenetic therapy can enhance tumor immunogenicity. A small number of clinical trial patients with advanced non-small cell lung cancer who initially received AZA and the HDACi Entinostat (MS275) and later moved on to α-PD-1 therapy had durable

responses compared to those who received α-PD-1 alone, suggesting that epigenetic therapy may somehow sensitize tumors to immune checkpoint inhibitors (64).

We support this hypothesis by finding, in a mouse model of ovarian cancer, that DNMTIs and HDACIs improve response to immune checkpoint inhibitors, through actions on both tumor and immune cells to reduce tumor burden and extend overall survival. This may stem, in part, from an AZA induced, interferon mediated, upregulation of an immune gene signature in both cell types, including genes involved in viral defense, chemokines, cytokines, interferon signaling, and cancer testis antigens (87,118). We show that inhibiting Type I interferon signaling by blocking the interferon α, β receptor 1 (IFNAR1) prevents the AZA mediated reduction in tumor associated ascites and eliminates the survival benefit for mice treated with AZA. Moreover, AZA treatment facilitates an increase in the number of CD45^{+} immune cells in the tumor microenvironment and leads to activation of CD8^{+} T cells and natural killer (NK) cells, which is reduced with IFNAR1 antibody blockade. While HDACIs are not effective as single agents, when combined with AZA *in vivo*, these drugs act on the immune compartment to improve the activation of CD8^{+} T cells, natural killer (NK) cells, and to decrease myeloid cells to create a less immunosuppressed tumor microenvironment. Together, the actions of these drugs on tumor cells and the tumor microenvironment indicate that epigenetic therapy may offer an approach to optimize immune checkpoint therapy for patients with ovarian cancer, and that the combination of AZA, the HDACi Givinostat (ITF2357, ITF), and α-PD-1 may hold the most promise.

Methods

Cell culture treatments

MOSE ID8-Defb29/Vegf-a (ID8-VEGF-Defensin) cells, kindly provided by Dr. Chien-Fu Hung, Johns Hopkins Pathology, which tested negative for mycoplasm in December 2016, were grown in RPMI medium, and treated with AZA (500nM). The A3 treatment

paradigm had AZA in the media on days 0, 1 and 2, while the A10 paradigm was also treated with AZA on days 3, 6, 7, 8 and 9. Cells were split on days 3 and 6, and harvested on Day 10 (A3 and A10).

Entinostat (MS275) treatment followed the AZA paradigms above, but with 100nM MS275 for 3 days, or 30nM MS275 for 3 or 10 days (HDACi3 or 10).

For the sequential combination of AZA and HDACi treatment, cells were treated with the A10 paradigm described above, followed by 3 doses of 100nM MS275 or ITF. The cells were collected on day 17 (AZA17, HDACi17, and AZA+HDACi17, Figure 3.1A). AZA (Sigma) was suspended in 0.9% saline. Entinostat (Syndax Pharmaceuticals) and Givinostat (SelleckChem) were both suspended in DMSO and diluted 1:1000 in media, so that the percentage of DMSO did not exceed 0.1%

Gene Expression Analysis

RNA extraction, RNA quality analysis, hybridization to Agilent 4x44k Human Gene Expression v2 arrays (Agilent Technologies) and analysis of the arrays were done as previously described (87). In some cases, tumor cells were isolated from ascites fluid by FACS and RNA was isolated using the Qiagen RNeasy Micro Kit (cat. no. 74004). After total cellular RNA was extracted using the Trizol method (Life Technologies, Carlsbad, California), RNA concentration was determined using the Nanodrop machine and software (Thermo Fisher Scientific, Rockville, Maryland). 1 µg total RNA was used to generate cDNA with the QuantiTect Reverse Transcription Kit (Qiagen, Venlo, The Netherlands). Quantitative reverse transcription PCR (q-RT-PCR) of ISG15, IFIT1, and ICAM1 mRNA was performed using TaqMan assays or Custom Taqman Gene Expression Array Cards (Life Technologies, Carlsbad, California) and the Applied Biosystems 7500 Fast real-time PCR system and software. TBP and was used as a reference gene. The ΔΔCT method was used to calculate relative expression levels.

Reverse transcriptase negative cDNA synthesis reactions were performed for at least one sample per plate.

Mouse endogenous retrovirus and SINE qPCR

Cells with A10 treatment were collected on days 3, 4, 7, and 10. RNAs were DNAseI treated and cDNA synthesis was performed (High-Capacity cDNA Reverse Transcription Kit, ThermoFisher). Expression of 9 mERVs genes (two IAP gag genes, an IAP-LTR, Mtv 7/8/9 sequences specific for C57Bl/6 mouse strains, and placental mERVs including syncytin-A, mErv-3, Peg11 and Mart8) and the B1 SINE gene was quantified by qPCR (ABI 7300) (see Supplemental Table 3.1 for primer sequences and q-PCR methodology). Mouse housekeeping genes:18S rRNA, β-actin and GAPDH were used for normalization (Supplemental Table 3.1). Ascites tumor cells were sorted using FACS at week 4.5 following *in vivo* AZA treatment (Supplemental Figure 3.6A). We examined gene expression for all 9 mERVs and B1 SINE gene expression in sorted ascites tumor cells. The full qPCR protocol was previously described(167),(168).

All mouse experiments

Tumor burden was assessed via measurement of body weight and amount of ascites drained from the mice at the point where they had gained 20-30% of their body weight. Statistical outliers were removed using Pierce's criterion. Mice were cared for in accordance with the policies of the JHU ACUC. n=10 mice for all treatment groups.

Mouse experiments with *ex vivo* epigenetic treatment of cancer cells.

Single agent therapy: 2.5×10^5 cells (A10) or 5×10^5 cells (HDACi3, HDACi10, and A3) were injected i.p. into 8-10 (A10) or 6-8 (HDACi3, HDACi10, and A3) week old female

C57Bl/6 mice. Immune cells were isolated from the ascites fluid via a Percoll gradient, and stained for FACS.

Combination therapy: $2.5x10^5$ cells treated with A17, HDACi17, or A+HDACi17 schedules were injected i.p. into 8-10 week old female C57Bl/6 mice. All cells from the ascites fluid were filtered and stained for FACS.

Mouse experiments with *in vivo* treatment

$2.5x10^5$ ID8-VEGF-Defensin cells were injected i.p. into 8-10 week old female C57BL/6NHsd (C57Bl/6) mice or NOD.Cg-*Prkdc^scid Il2rg^tm1Wjl*/SzJ (NSG) mice 3 days after injection. 0.5mg/kg AZA or saline was given i.p., for 5 days a week. The following week, 2mg/kg Givinostat or Entinostat or 1% DMSO in saline was injected i.p. for 5 days. For the rest of the experiment, the treatment alternated AZA/HDACi every other week. α-PD-1 (200ug/mouse) was given on days 17, 20, 24, and 27 after injection in the C57Bl/6 mouse experiment. α-PD-1 (1mg/mL in saline) was kindly provided by Dr. Michael Lim of the SKCCC, Johns Hopkins University. Blocking of IFNAR1 was achieved with the anti-mouse IFNAR1 antibody (clone MAR1-5A3), injected every 3 days (0.5mg/mouse)(169). Anti-IFNAR1 and the mouse IgG isotype control were purchased from Leinco Technologies and diluted in PBS.

Flow cytometry

Ascites were drained or spleens were collected from 5-10 mice per group and incubated in ACK buffer (Thermo Fisher) to lyse red blood cells for 10 minutes, then washed. Ascites from each mouse was individually lysed and prepared for flow cytometry. Mononuclear cells collected were cultured for 4 hours in RPMI with 5% Fetal Bovine Serum and in the presence of Cell Stimulation Cocktail (plus protein transport inhibitors; eBioscience). Cells were then washed and stained for cell surface markers including

Live/Dead (eBioscience), CD45 (BD Biosciences), CD3 (BD Biosciences), CD4 (BD Biosciences), CD8 (BD Biosciences), PD-1 (eBioscience), NK1.1 (BD Biosciences), F4/80 (Biolegend), MHC II (Biolegend, Isotype Control #400627), GR1 (Biolegend, Isotype Control #400635), and CD11b (Biolegend). After incubation, the cells were permeabilized (FoxP3 staining buffers, eBioscience). Intracellular staining was performed for FoxP3 (eBioscience, Isotype Control #12-4321) and IFNγ (BD Biosciences, Isotype Control #554686). Flow cytometry acquisition was performed on an LSRII cytometer (BD Biosciences) and data were analyzed using FlowJo software version 10.2.

Chemokine and Cytokine Array

Cultured cells were treated with an A10 treatment schedule and media was collected at day 10. Ascites from mice treated with AZA as described above was collected at week 4 after injection of cells. Cells were removed from ascites and supernatant collected. Media and ascites samples were analyzed with the Proteome Profile Array, Mouse Cytokine Panel A (R&D Systems) according to manufacturer instructions.

Cell Cycle and Apoptotic Analysis

Cells were treated with an A10 treatment schedule and collected on Days 3 and 10.   For cell cycle analysis, BrdU (10uM, Sigma) was incubated with cells for 2 hours. Cells were fixed, treated with DNase (300ug/mL), and stained with anti-BrdU (Biolegend) and 7-AAD (Life Technologies). For apoptosis analysis, cells were stained for FACS and were measured as apoptotic based on positive Annexin V (eBioscience) and 7-AAD (Life Technologies) staining. Flow cytometry was performed on a FACS Calibur cytometer (BD Biosciences) and data were analyzed with FlowJo V10 software.

Western Blots

Protein extracts were quantified and immunoblotted using the 4%–20% Mini-PROTEAN TGX gel system (Bio-Rad) and PVDF membranes (Millipore). β-actin or GAPDH was used as a loading control. Antibodies used were as follows: polyclonal rabbit anti-mouse cleaved PARP (Cell Signaling, 1:1000), polyclonal rabbit anti-DNMT1 (Sigma, 1:1000), mouse anti-β-Actin (Sigma, 1:10,000), and polyclonal rabbit anti-GAPDH (Trevigen, 1:10,000). Band intensities were quantified using the program Adobe Photoshop Elements 6.0.

RNA extraction and sequencing library generation for immune cells

CD8$^+$ and CD4$^+$ T cells and CD11b$^+$ myeloid cells were sorted using a FACS Aria II from ascites derived from mock and AZA treated mice. Approximately 10,000 cells were collected for each sorted population, based on viability, size- and lineage-exclusion. Cells were pelleted at 300 x g for 10 mins. The supernatant was carefully removed and 100 µL of Arcturus PicoPure extraction buffer (ThermoFisher Scientific) was added. Total RNA was extracted using Arcturus PicoPure RNA isolation kit according to the manufacturer's protocol. Low-input RNA sequencing libraries were generated from 200 pg of total RNA using SMART-seq v4 Ultra Low Input RNA kit (Clontech). All samples were subjected to 13 PCR amplification cycles to minimize PCR biases. Amplified cDNA libraries were later fragmented through sonication to obtain 200 – 500 bp fragments. Standard Illumina sequencing libraries were prepared using Rubicon ThruPLEX DNA-seq kit (Rubicon Genomics) according to manufacturer's protocol. Sample barcoded libraries were sequenced on Illumina's NextSeq 500 instrumentation using NextSeq 300 Cycle Kit, High Output, V1 reagents (Illumina) and data analysis workflow, bcl2fastq - v2.17.1.14, to obtain 150 bp paired-end reads.

Paired-end RNA sequencing reads were trimmed to remove Illumina's adapter

sequences. Sequencing reads were further processed to remove poor quality reads

and/or reads mapping to mouse rRNA and tRNA sequences using ArrayStudio package

(www.omicsoft.com/array-studio). Following criteria was used to remove poor quality

reads: Trim reads with base quality score (Sanger Quality Score) <10; Filter out reads if

trim length is < 25 bp; Filter out reads if maximal base quality score is < 15, Filter out

reads if average quality score is < 10; Filter out reads if poly AGCT rate is >= 80%; Filter

out the pair if either read fails the filtering criteria. Sequencing reads were aligned to the

mouse reference genome (Build38) using OSA version 4 (PMID: 22592379). To obtain

transcript counts data, RSEM package (PMID: 21816040) and NCBI mouse RefSeq

gene model (release July 2015) annotations were used. Transcripts with zero counts in

more than two third of the samples were discarded from downstream analysis to reduce

noise in the expression data. Filtered counts data was later normalized using quantile

normalization and differentially expressed transcripts were identified using Limma Voom

(PMID: 24485249). A p-value cutoff of 0.05 was used to classify transcripts as

differentially expressed in treatment condition. Upstream regulator and pathway

analyses on differentially expressed transcripts were performed using QIAGEN's

Ingenuity Pathway Analysis (www.qiagen.com/ingenuity).

Statistical Analysis

Data was graphed in GraphPad PRISM 5.0, and significance was determined by a

Mann-Whitney t-test or by multiple pairwise comparisons using the one-way ANOVA test

with Bonferroni Correction. Significances in survival data were determined by Mantel-

cox (log rank) test. Differences were deemed significant with a p-value of less than 0.05.

Outliers were removed from ascites volume data sets and ascites immune cell data sets

using the Peirce's Criterion (170) Significances are shown with p<0.05 (*); p<0.01 (**) or p<0.001 (***).

Results

Pre-treatment of tumor epithelial cells *ex vivo*

To study how DNMTIs and HDACIs directly affect tumor epithelial cells to regulate response and immune cell interactions, we pre-treated cultured, syngeneic mouse ovarian surface epithelial cancer cells, ID8-VEGF-Defensin (131-134), with epigenetic agents, injected the cells into untreated mice, and analyzed ascites volume as a measure of tumor burden (152). Ten or 17 (A10, A17), but not 3 (A3-10), days of AZA pre-treatment of tumor cells led to significantly less ascites (Figure 3.1B), reflected as a reduction in weight gain (Supplemental Figure 3.1A), and increased mouse survival compared to vehicle (Mock) or HDACi pre-treated tumor cells (Figure 3.1A-D, Supplemental Figure 3.1A, B). Combination pre-treatment of AZA and Entinostat (A+MS17) or AZA and Givinostat (A+ITF17) decreased ascites compared to mock, but did not decrease ascites (Figure 3.1C) or improve survival (Figure 3.1D) over AZA treatment alone. Overall, the decrease in ascites volume and increase in survival with AZA or AZA+HDACi pre-treatment appears to be driven by an AZA mediated effect on tumor cells.

AZA pre-treatment of tumor epithelial cells in these *ex vivo* treatment studies led to changes in the immune microenvironment with increased numbers of immune cells (CD45$^+$) in the ascites of A10 pre-treated tumor cells (Figure 3.2A, B). Neither the addition of Givinostat (A+ITF17), nor Entinostat (A+MS17), to AZA increased the number of CD45$^+$ cells above AZA alone (Figure 3.2C). Pre-treatment with AZA (A17) also changed the percentages of immune cell subsets, including increasing the percentage of NK cells, activated NK cells, and dendritic cells, and decreasing the percentage of

40

macrophages (Figure 3.2D-H). HDACi pre-treatment alone or in combination with AZA did not generally cause or increase the aforementioned changes (Figure 3.2C-K). The effects of AZA pre-treatment are still observed 4-5 weeks after treatment, suggesting a long-lasting AZA mediated effect on the tumor cells, which may then signal to untreated host immune cells.

AZA induced immune signaling in tumor cells

Treatment with AZA at doses that degrade its molecular target, DNA methyltransferase 1 in ID8-VEGF-Defension cells (Supplemental Figure 3.1C, D, E) caused an upregulation of an immune related viral defense signature in these murine cells, as was previously described for human ovarian cancer cells (118), (Supplemental Figure 3.2A). This expression, also seen in cancer testis antigens (CTAs), was especially robust with prolonged treatment (Supplemental Figure 3.2A, B). HDACIs have been shown to synergize with DNMT inhibitors to re-express silenced genes in cancer (16,51), but Entinostat (MS275) or Givinostat (ITF) treatment (HDACi17) alone or in combination with AZA caused only small or moderate changes in the expression of the antiviral and CTA genes in these mouse ovarian cancer cells (Supplemental Figure 3.2C, D).

We previously demonstrated that AZA treatment of human ovarian carcinoma cell lines induced the expression of RNA from endogenous retroviruses (ERV), which led to increased interferon signaling and viral defense gene expression (118,119). We now demonstrate in mouse ovarian ID8-VEGF-defensin cells that AZA significantly increased several mERVs in both cultured tumor cells (Supplemental Figure 3.2E) and tumor cells sorted from ascites from treated C57Bl/6 mice (Supplemental Figures 3.2F, 3.6A, Supplemental Table 3.1).

Lastly, AZA treatment *in vitro* (A10) and *in vivo* (Supplemental Figure 3.6A) increased the secreted protein levels of chemokines and cytokines. Of the 9 increased in cultured cells, only CXCL10, CXCL1, and CCL2 were also increased in the ascites fluid (Supplemental Figure 3.2G, H).

Treatment of mice with AZA, HDACi, and α-PD-1

Having shown that pre-treatment of ovarian tumor cells led to increased immune cells in the tumor microenvironment and improved survival of the mice, we next asked whether the addition of α-PD-1 would provide added benefit. Mice bearing ovarian tumors treated intraperitoneally with AZA, an HDACi, and α-PD-1 had improved overall survival, decreased tumor burden, and alterations of immune cell populations that would promote immune cell killing of tumor cells (Figure 3.3, 3.4). AZA as a single agent or in combination with either HDACi or α-PD-1 significantly reduced ascites volume (Figure 3.3B, expansion), while HDACIs or HDACIs+α-PD-1 were ineffective (Figure 3.3B). Mirroring these ascites data, α-PD-1, HDACIs alone, or HDACIs plus α-PD-1 did not affect survival (Supplemental Figure 3.3B), while the combination of AZA with either HDACi significantly improved this key parameter over AZA treatment alone (Figure 3.3C). This is in contrast to the *ex vivo* treatment model, where the addition of HDACi to AZA did not affect the tumor burden or overall survival. The improved survival with *in vivo* treatment may reflect the effects of the epigenetic drugs on the host immune cells. Adding α-PD-1 to AZA+ITF further significantly increased survival over AZA+ITF or AZA+MS+α-PD-1 (Figure 3.3D-F. In summary, the triple combination of AZA+ITF+α-PD-1 was the most effective at decreasing ascites volume and increasing overall survival (Figure 3.3F).

Immune cell populations in the ascites fluid of tumor bearing mice were changed by epigenetic therapy and α-PD-1, but immune cells in non-malignant tissues, such as the spleen, were not affected (Supplemental Figure 3.6B). AZA treatment moderately but significantly increased the percentage of activated CD4+ and CD8+ T cells and NK cells in the tumor microenvironment, and, when combined with ITF or either HDACi and α-PD-1, this activation was markedly enhanced (Figure 3.4A, B, C). All treatments containing AZA led to an increase in the percentage of T cells (Figure 3.4D), though this effect was less consistently observed in replicate experiments than the increases in activation of CD8+ T and NK cells. None of the treatment groups altered the percentages of T regulatory, CD4+, CD8+, CD4+PD-1+, or CD8+PD-1+cells, or the CD4/CD8 ratio (Supplemental Figure 3.4), The addition of Givinostat or either HDACi+α-PD-1 to AZA therapy increased the activation of key tumor-killing subsets of immune cells.

Myeloid derived suppressor cells, which aid in tumor immune evasion (171), were significantly decreased by almost all therapies, with the exception of ITF and ITF+α-PD-1; however, this exception may be due to limitations in sample number and high variability (Figure 3.4E). All treatments containing AZA decreased the percentage of macrophages, which can influence tumor growth (172) (Figure 3.4F). Compared to AZA alone, the addition of an HDACi significantly decreased the percentage of macrophages further. Overall, increased numbers of CD45+ immune cells, increased activation of CD8+ T cells and NK cells and decreases in macrophages and MDSCs were the most consistent, significant changes resulting from epigenetic therapy.

In support of the fact that *in vivo* epigenetic treatment alters host immune cell populations in the tumor microenvironment, we find that AZA treatment increases expression of viral defense genes in CD8+ and CD4+ T cells and in CD11b+ myeloid cells in the ascites fluid of treated, tumor bearing mice (Supplemental Figure 3.5 A,B). Ingenuity analysis also identified interferon associated genes as top upstream regulators

of the transcriptional program in these *in vivo* AZA treated cells (Supplemental Table 3.2). These results suggest that the AZA induced increase in gene expression of interferon associated genes in both tumor and host immune cells may be an integral component of the improved outcome of mice treated with epigenetic therapy and immune checkpoint inhibitors.

In summary, the combinations of epigenetic agents, as well as the addition of α-PD-1 to AZA+HDACi, increase the numbers and activation of key tumor killing immune cells to the tumor microenvironment and decrease numbers of MDSCs and macrophages (Figure 3.4). We hypothesize that these effects contribute to the reduction in tumor burden and survival when treating with AZA, its combination with HDACIs, and importantly these agents combined with α-PD-1.

Blockade of IFNAR1 inhibits the actions of AZA

Our expression data show that AZA treatment leads to increased interferon signaling and viral defense gene expression in ID8-VEGF-Defensin cells (Supplemental Figure 3.2A,C). We therefore questioned the role and importance that interferon signaling plays in the AZA induced decrease in tumor burden and alterations in immune cells observed in Figures 3.3 and 3.4. To test this hypothesis, we injected α-IFNAR1 (i.p., 0.5mg/kg) every 3 days into mice harboring ID8-VEGF-Defensin tumor cells, simultaneously treated with AZA or vehicle control (Mock) (Figure 3.5A). The AZA mediated reduction in ascites volume routinely observed in our experiments was inhibited by treatment with anti-IFNAR1 (Figure 3.5B) and total numbers of CD45$^+$ cells in the ascites were not increased as with the AZA treatment, but remained near mock values (Figure 3.5C). Likewise, activation of CD8$^+$ T effector cells and natural killer (NK) cells in response to AZA treatment was also completely blocked and rescued by anti-IFNAR1 (Figure 3.5D, E) and there was no survival benefit for mice treated with AZA

and anti-IFNAR1 (Figure 3.5F). As expected, antibody blockade of IFNAR1 *in vitro*

prevented the AZA induced increase in expression normally observed for anti-viral

genes, such as ISG15, IFIT1 and ICAM1 (Figure 3.5G, H, I). Previous *in vitro* studies

have demonstrated that upregulation of a dsRNA sensing pathway by AZA triggers the

activation of an intact Type I interferon signaling pathway requiring the interferon alpha

and beta receptor subunit 1 (118,119). Our α-IFNAR1 data are the first to indicate that

the type I interferon response is, indeed, required for effective *in vivo* anti-tumorigenic

actions of 5-Azacytidine, including reduced tumor burden, extended survival, and

increased numbers and activation of immune cells. .

AZA+HDACi efficacy requires a treated immune system

       To assess the role of the immune cells in the anti-tumorigenic response, we

compared the response to epigenetic agents in treated immune-deficient NSG mice that

lack functional B, T and NK cells (173) (Figure 3.6A) to the response in the treated

immunocompetent mice (Figure 3.3). In the NSG immunodeficient mice, AZA treatment

reduced ascites volume and increased survival as in the C57Bl/6 mice, and HDACi

treatment alone did not significantly affect ascites volume or survival in either mouse

model. Combination treatment was more effective than AZA as a single agent in the

treated immune competent C57Bl/6 mice (Figure 3.6B, C), and not in the

immunodeficient mice or in the pretreatment model (Figure 3.1), suggesting that when

combined with AZA, HDACIs may act on the immune microenvironment to reduce tumor

burden. Taken together, these data imply that AZA can act on both tumor and immune

cells, while the added benefit of the combination with the HDACi may rely on the

treatment and presence of an intact host immune microenvironment. Specifically, the

activation of T and NK cells and decreases in macrophages were all significantly

enhanced by the HDACi addition to AZA and may be responsible for the reduction in

tumor burden in the treated mice in an immune intact setting (Figure 3.4B, C, D, F).

AZA has direct anti-tumorigenic effects

In the absence of tumor killing immune cells in the NSG model, it was intriguing that we noted increased numbers of dead cells in the CD45$^-$ (non-immune cell) population with AZA and AZA+ITF treatment, the two groups with the longest median survival (Figure 3.6D). This could be explained by the fact that the anti-tumor effects of AZA can be mediated through mechanisms that are not immune related, such as apoptosis and disruption of the cell cycle (118,155-157). Indeed, three or 10 days of *in vitro* treatment of the tumor cells (A3-3, A10) with 500nM AZA caused a significant decrease in cultured cell numbers (Figure 3.7A, B) associated with signs of apoptosis reflected by increased cleaved-PARP protein levels and percentage of cells positive for Annexin V and 7-AAD (Figure 3.7C, D, E, F). These data confirm that nanomolar doses of AZA induce a low level of apoptosis in cancer cells, as we have previously described (118,155), which appears to be too small to account for the large decrease in tumor cells observed in culture (Figure 3.7B). A more important factor in the decrease in tumor cell number could be that A3 and A10 treatment *in vitro* decreased the percentage of tumor cells in S phase and increased those in G2-M arrest (Figure 3.6G, H), as has been observed in other models (156,157). In summary, AZA directly affects intrinsic, anti-tumorigenic mechanisms in the tumor cells, leading to increased apoptosis and cell cycle arrest.

Overall, our data demonstrate that AZA reduces tumor burden and increases the number of immune cells in the tumor microenvironment, in part through effects on the tumor cells themselves. AZA treatment upregulates immune gene expression in tumor cells and in immune cells, and type 1 interferon signaling is required for some anti-tumorigenic effects of *in vivo* AZA, such as decreased ascites burden, extended survival, and activation of immune cells. When tumor bearing mice are treated *in vivo*, the

addition of an HDACi to AZA further reduces tumor burden and increases survival,

perhaps due to an increase in activated T and NK cells and a decrease in macrophages.

Finally, the combination of AZA, Givinostat, and α-PD-1 was the most effective in

improving overall survival.

Discussion

The use of different treatment models in this study has enabled us to understand

how 5-azacytidine (AZA) and HDACIs act individually and in combination on ovarian

tumor epithelial cells and immune cells in the microenvironment to establish anti-tumor

responses and to enhance immune checkpoint therapy. Low doses of AZA, but not

HDACIs, directly induce multiple anti-tumorigenic mechanisms in tumor cells, most

notably increased immune signaling, increased apoptosis, and disruptions of the cell

cycle. However, when an HDACi, especially Givinostat, is combined with AZA *in vivo* so

that both tumor and cells in the immune microenvironment are exposed to the drugs,

these agents can enhance the activation of specific immune subsets such as T and NK

cells. Our data now show that that the addition of an HDACi to a DNMTi may be optimal

to achieve a maximal sensitization to checkpoint inhibitors. The addition of Givinostat,

but not Entinostat, to AZA was able to sensitize the tumors to α-PD-1 therapy. The

reasons why Givinostat outperforms Entinostat in overall survival when combined with

AZA and α-PD-1 are currently under investigation. Other studies have shown that

HDAC inhibition can affect tumor associated immune cells, with one finding that B cells

as well as interferon-γ receptor signaling in the tumor cells were important for the anti-

tumorigenic effect of the HDACIs vorinostat and panobinostat in syngeneic models of

colon cancer and lymphoma (126).

In our study, blockade of type 1 interferon signaling through an antibody against

IFNAR1 impairs the anti-tumorigenic effects of AZA. Although it had been observed that

AZA treatment could stimulate interferon pathway induction by the viral defense pathway signaling, it was not known what *in vivo* consequences would be linked to this pathway upregulation. Importantly, our data now demonstrate that many of the anti-tumorigenic actions of AZA in ovarian cancer are mediated via the interferon α, β receptor subunit 1, including decreased tumor burden, increased CD45^{+} immune cells in the tumor microenvironment, and increased activation of CD8^{+} T and NK cells.

In addition to the effects on immune cells described above, we hypothesize that AZA mediated apoptosis and cell cycle disruptions in ID8-VEGF-Defensin cells may also be dependent on IFNAR1 signaling. *In vitro,* AZA has been shown to lead to increases in apoptosis and decreases in self renewal that can be rescued by inhibiting the interferon response (118,119). In response to anti-IFNAR1 *in vivo*, ascites volume in AZA treated mice remained similar to mock values (Figure 3.5B), and did not show the decrease in ascites volume that was observed with AZA treatment in the NSG mice (Figure 3.6), suggesting that anti-IFNAR1 inhibition of interferon signaling may also prevent apoptosis and blocks in cell cycle.

Others have tested whether the interferon response can play a role in sensitization to immune checkpoint blockade, as stabilization of IFNAR1 improves efficacy of anti-PD-1 therapy (123), and the loss of interferon gamma pathway genes is a mechanism of resistance to anti-CTLA-4 (124). On the other hand, prolonged tumor interferon signaling has been shown to induce resistance to immune checkpoint blockade over time (125), implying that perhaps the timing and duration of the response is important. Our study provides a greater understanding of how interferon signaling may sensitize tumors to immune checkpoint blockade.

The AZA induced increases in immune signaling observed in ID8-VEGF-defensin mouse ovarian cancer cells are consistent with our results for AZA treated human ovarian cancer cells (87,118). Thus, in both the human and murine tumor cells, AZA

48

treatment leads to an increase in the expression of endogenous retroviral transcripts (ERVs), viral defense genes, cancer testis antigens and chemokines/cytokines (87,118,119). Chemokines CXCL10, CXCL1, and CCL2 were detected in both the cell culture media of AZA treated murine cells and the ascites fluid of AZA treated mice. CXCL1 and CCL2 have been identified in patient ascites (174) and CXCL10 in humanized models of ovarian cancer (97), validating the relevance of the ID8-VEGF-defensin mouse model of ovarian cancer to human disease, and suggesting that these chemokines/cytokines may play a role in the AZA induced recruitment of immune cells to the tumor associated ascites(175-177).

Our studies now provide mechanistic insight for previous studies showing that epigenetic agents may alter the tumor associated microenvironment to potentially sensitize tumors to immunotherapy (94,95,97,118,129). In a previous study, treatment with the DNA demethylating agent decitabine increased the percentage of activated NK and CD8$^+$ T cells in the ascites fluid with associated improvement of the efficacy of anti-CTLA-4 immunotherapy and longer survival of the mice (96). In another ovarian cancer study, inhibition of DNMT1 and the epigenetic repressor EZH2 increased tumor expression of T helper 1 (T$_H$1)-type chemokines CXCL9 and CXCL10. This change in immune signaling from the tumor led to increased tumor infiltrating T Effector cells, inhibited tumor growth, and increased the sensitivity of the tumor to adaptive T cell transfusion therapy or PD-L1 blockade (97). Our study now defines the cellular targets of AZA and HDACIs using a more comprehensive panel of immune cells and proving a requirement for Type I interferon signaling in the AZA-induced immune response. We have shown that the addition of an HDACi to AZA can increase the activation of immune subsets, using doses of epigenetic therapy that are clinically relevant and can be immediately applied in clinical trials. The preclinical data in this manuscript helped to initiate a Celgene sponsored, Phase II Randomized Study of Pembrolizumab With or

Without Epigenetic Modulation With CC-486 (Oral AZA) in Patients With Platinum-resistant Epithelial Ovarian, Fallopian Tube or Primary Peritoneal Cancer (178). This trial started enrollment December 2016 and will hopefully reveal that addition of a DNMTi to checkpoint inhibitor therapy provides benefit beyond that of immunotherapy alone. The addition of an HDACi to the DNMTi in future trials may provide more benefit, and our data suggest that this combination will provide optimal sensitization to immune checkpoint blockade.

Figure 3.1: Pretreatment of tumor epithelial cells with AZA and transplantation into untreated C57Bl/6 mice leads to decreased tumor associated ascites and increased overall survival.
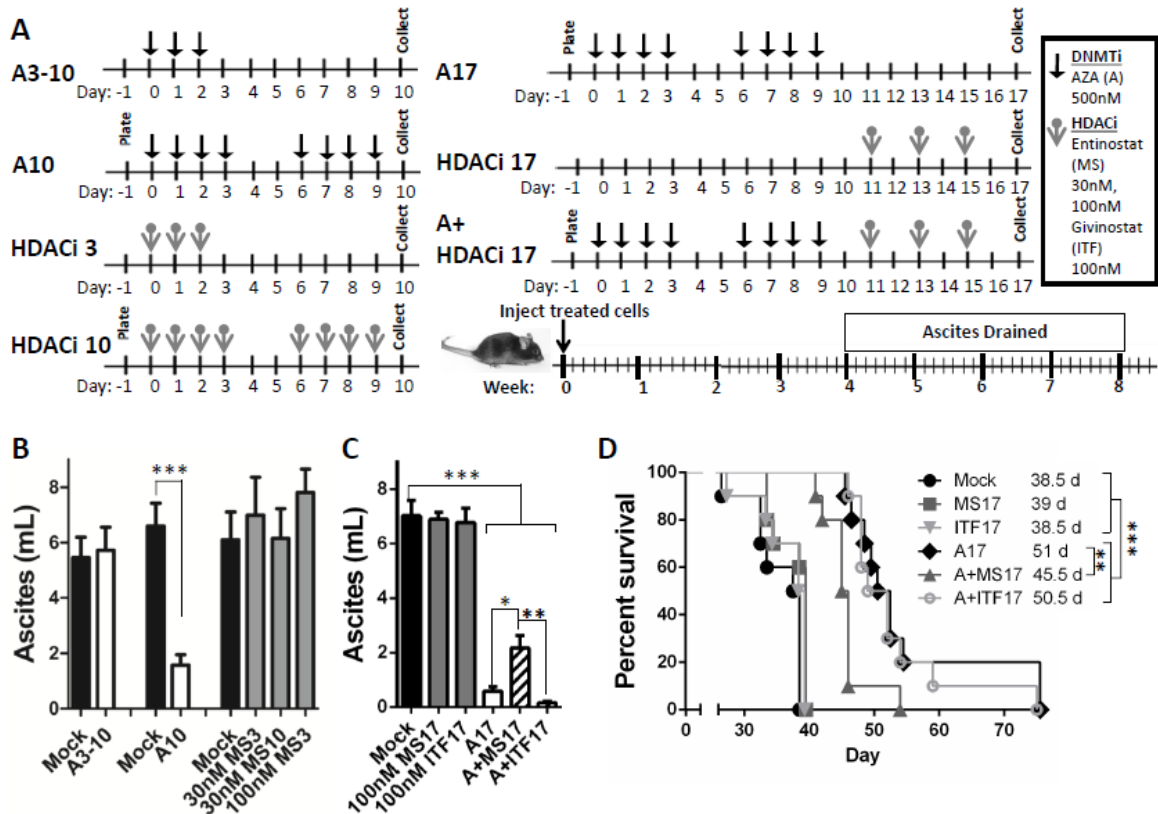
A) Treatment schematic for *in vitro* treatment of cultured ID8-VEGF-Defensin cells. **B-C)** Ascites volume drained from mice 4-5 weeks after pre-treated tumor injection. Mean+SEM is shown. A10, MS3, MS10: n=3; A3-10: n=2; MS17, ITF17, A17, A+MS17, and A+ITF17 n=1. Statistical outliers were removed using Pierce's criterion, and significance was determined by a Mann-Whitney t-test. **D)** Survival of mice in days, with median survival shown. Significance was determined using a log rank (Mantel-Cox) test.

Figure 3.2: Pretreatment of tumor epithelial cells with AZA and HDACi lead to alterations in the numbers and activation of immune cell populations in tumor associated ascites.
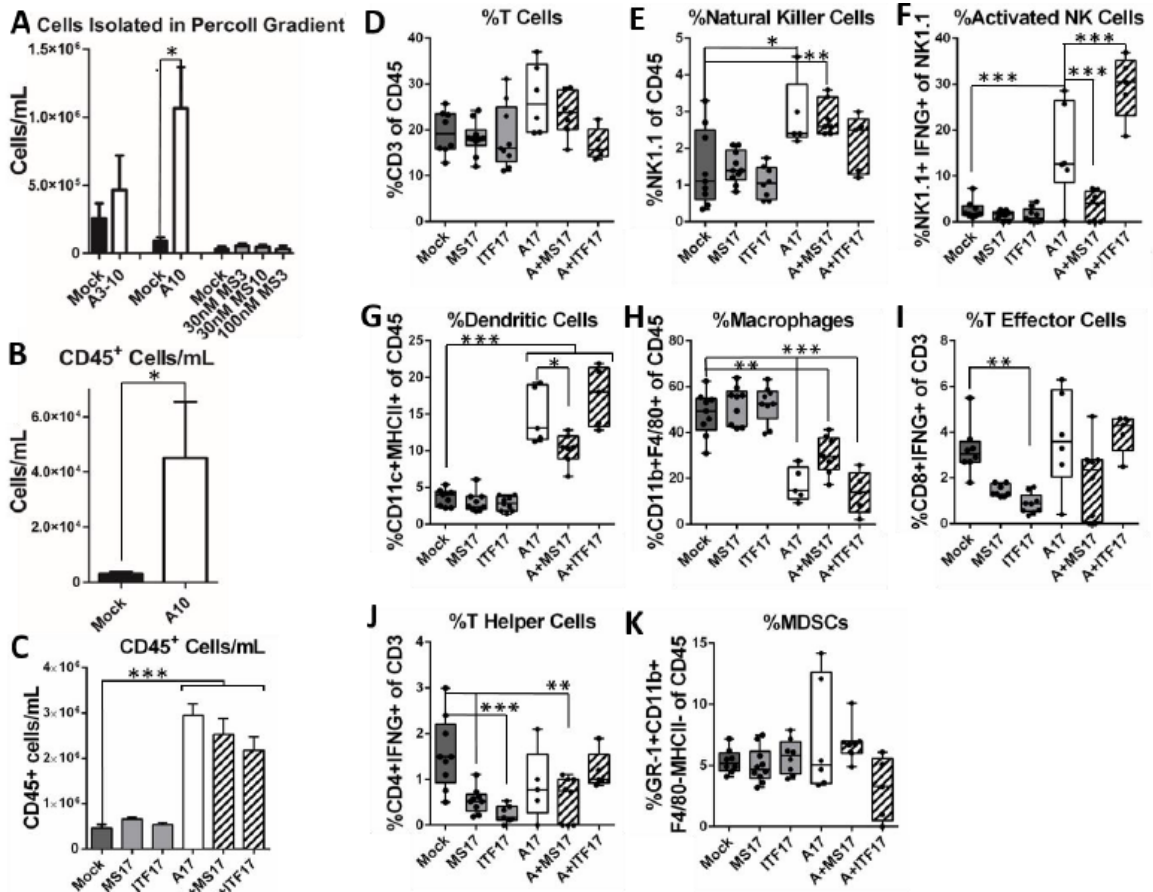
ID8-Vegf-Defensin cells were pretreated and injected into mice. Cells were analyzed from the ascites fluid drained (Figure 3.1A-C). **A)** Immune cells/mL isolated via Percoll gradient (n=2). **B)** CD45$^+$cells/mL identified via Percoll gradient and FACS (n=2). Mean+SEM is shown in A-B, and significances are determined by Mann-Whitney t-test. (**C-K**). All cells from ascites were analyzed via FACS (n=1). **C)** CD45$^+$ cells/mL of ascites. Mean+SEM is shown and significances are determined by one-way ANOVA. **D-K)** Median, 25th and 75th percentiles, and range are plotted and significances are determined by one-way ANOVA. **D)** %T cells (CD3$^+$) of CD45$^+$cells. **E)%**Natural killer cells (NK1.1$^+$) of CD45$^+$ cells. **F)** % Activated natural killer cells (NK1.1$^+$, IFNγ$^+$) of NK1.1$^+$ cells. **G)** %Dendritic cells (CD11c$^+$MHCII$^+$) of CD45$^+$ cells. **H)** %Macrophages (CD11b$^+$, F4/80$^+$) of CD45$^+$ cells. **I)** %T effector cells (CD8$^+$IFNγ$^+$) of T cells **J)** %T helper cells (CD4$^+$IFNγ$^+$) of T cells. **K)** %Myeloid derived suppressor cells (GR-1$^+$, CD11b$^+$, F4/80$^-$, MHCII$^-$) of CD45$^+$ cells.

52

Figure 3.3: The addition of immune checkpoint inhibition to epigenetic therapy in an intact mouse model decreases tumor burden and increases survival.
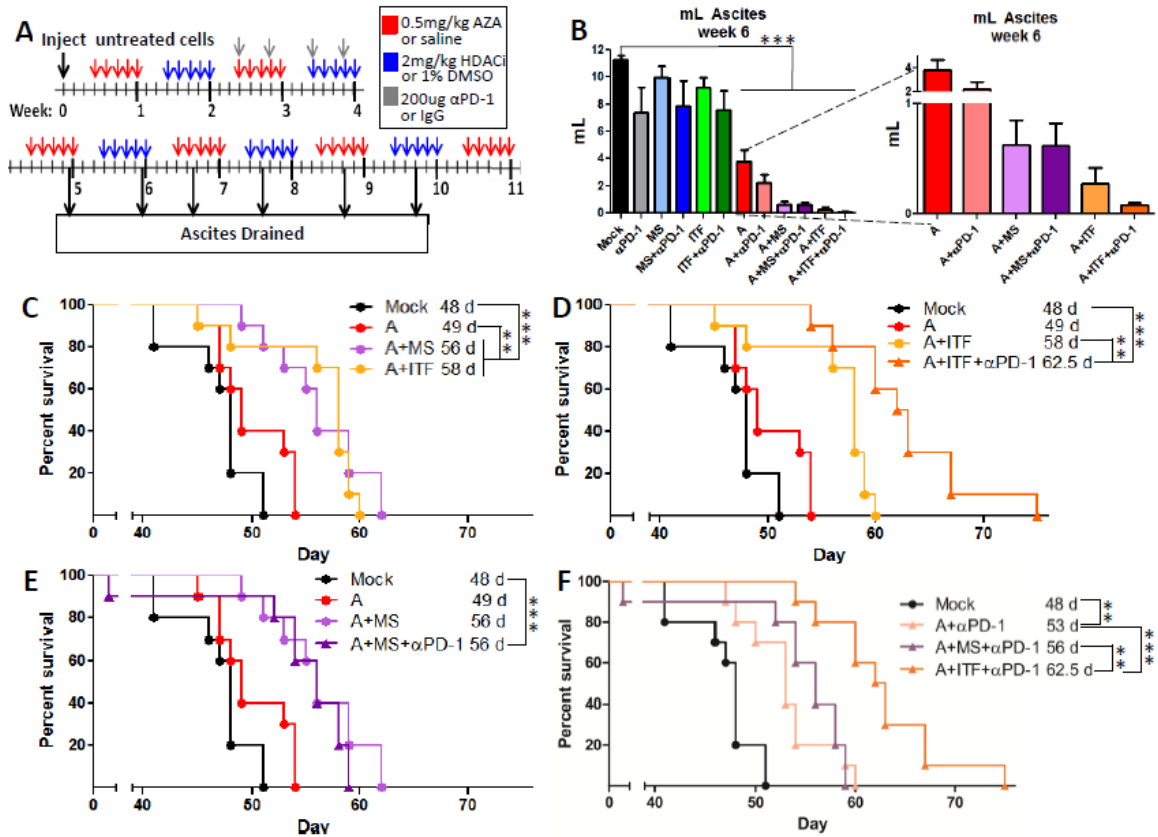
**A)** *In vivo* treatment schematic of AZA (A), Entinostat (MS), Givinostat (ITF) and α-PD-1. **B)** Volume of ascites fluid drained at week 6. Mean+SEM is shown and significances are determined by one-way ANOVA. All significances are compared to Mock, *=p<0.05, **=p<0.01, ***=p<0.001. **C-F)** Survival of the mice in days, with median survival shown. Significances are determined by log rank (Mantel Cox) test.

Figure 3.4: Epigenetic therapy and α-PD-1 increases the number and activation of immune cells in the tumor microenvironment.
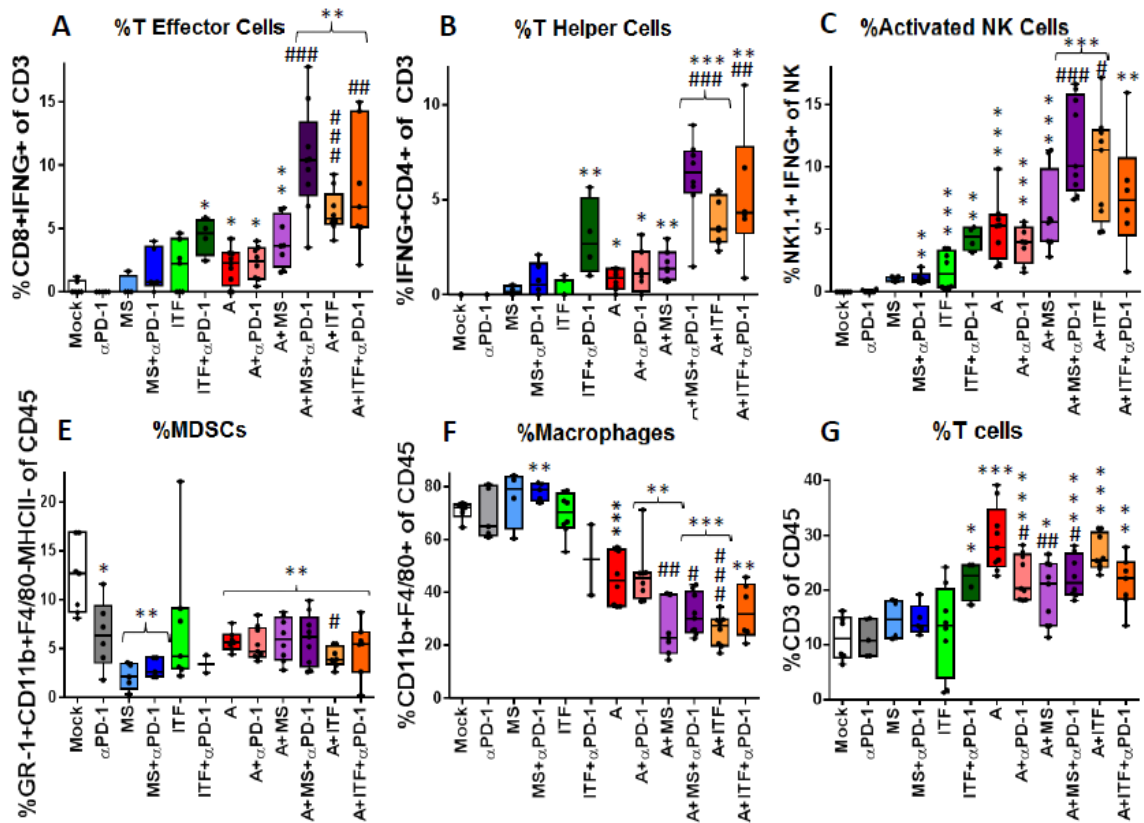
Mice were treated as described in Figure 3.3A. Cells from ascites fluid drained at week 6.5 were analyzed via FACS. Median, 25th and 75th percentiles, and range are plotted for each experimental arm and significances are determined by Mann Whitney T test. Significances compared to Mock are marked with *, and significances compared to AZA are marked with #. */#-p<0.05, **/##-p<0.01, ***/###-p<0.001. **A)** %CD3+ T cells of CD45+ cells. **B)** %T effector cells (CD8+IFNγ+) of T cells. **C)** %T helper cells (CD4+IFNγ+) of T cells. **D)** % activated NK cells (NK1.1+, IFNγ+) of NK1.1+ cells; **E)** %Myeloid derived suppressor cells (GR-1+, CD11b+, F4/80-, MHCII-) of CD45+ cells; **F)** %Macrophages (CD11b+, F4/80+) of CD45+ cells.

Figure 3.5: Blockade of IFNAR1 inhibits the actions of AZA.
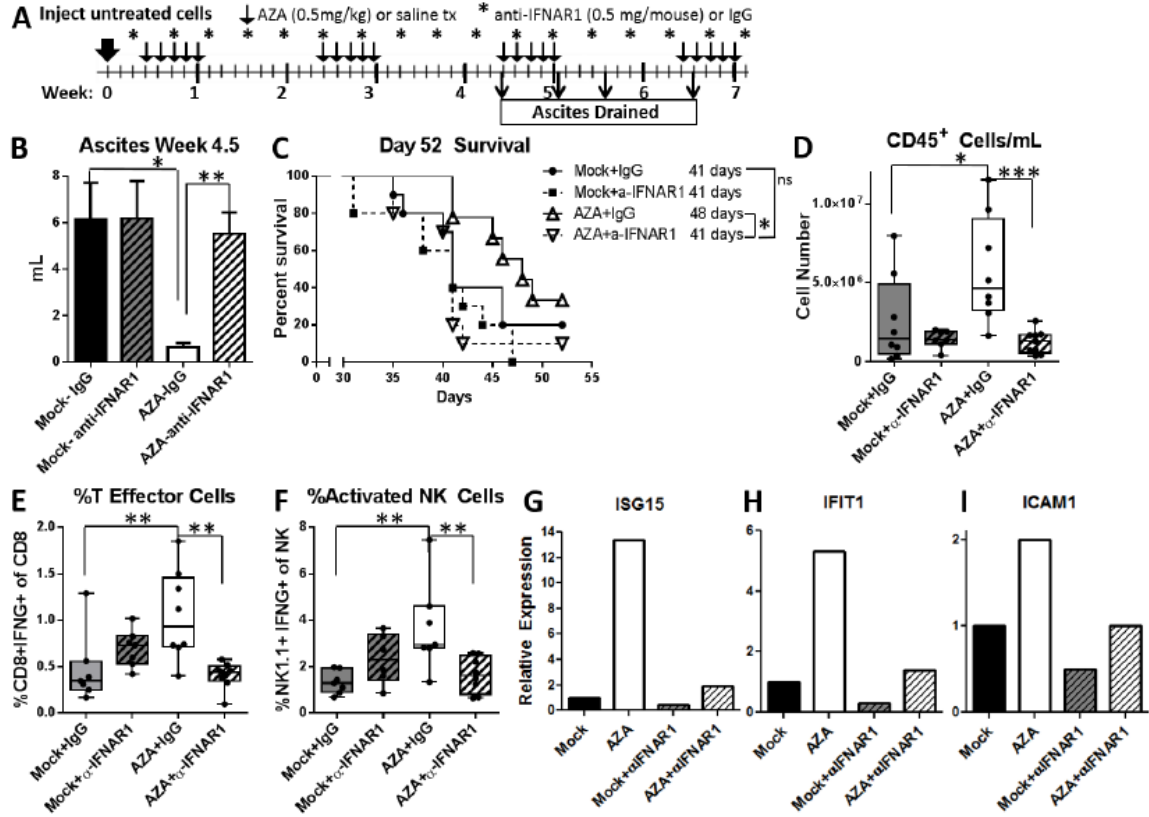
A) Treatment schematic for the mice. Mice were treated with AZA or saline as described in Figure 3.3. Anti-IFNAR1 was injected i.p. (0.5 mg/mouse) every three days, beginning one day before the AZA regimen. **B)** Volume of ascites drained from the mice at week 4.5. Mean+SEM is shown and significances are determined by Mann-Whitney T-test. **C)** Survival of the mice in days, with median survival shown. Significances are determined by log rank (Mantel Cox) test. **D-F)** Median, 25th and 75th percentiles, and range are plotted, and significances are determined by Mann-Whitney T-test. **D)** CD45$^+$ cells/mL of ascites. **E)** %T effector cells (CD8$^+$IFNγ$^+$) of CD3$^+$ T cells. **F)** % activated NK cells (NK1.1$^+$, IFNγ$^+$) of NK1.1$^+$ cells. **G-I)** Relative expression of interferon stimulated genes in cells treated with AZA and anti-IFNAR1 *in vitro*. AZA was given in an A3 treatment schedule, and one dose of anti-IFNAR1(10ug/mL) was given at day 0. Cells were collected at day 3 for expression analysis via qRT-PCR.

Figure 3.6: AZA+HDACi combination therapy is less effective at reducing tumor burden and increasing survival in an immunodeficient mouse model.
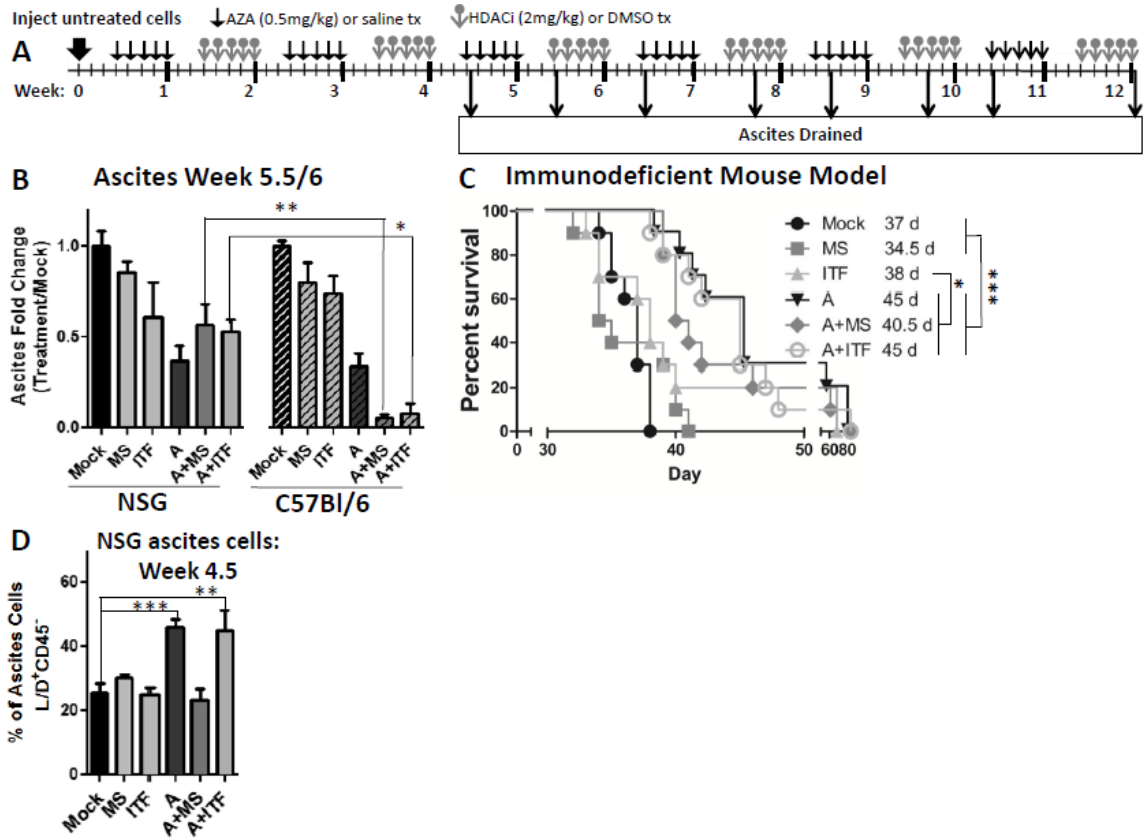
A) Treatment schematic for *in vivo* treatment of NSG mice with AZA (A) and HDACIs Entinostat (MS) or Givinostat (ITF). **B)** Fold change in ascites volume drained at week 5.5 (NSG) or 6 (C57Bl/6). The C57Bl/6 data from Figure 3.3A is shown here for direct comparison. **C)** NSG mice survival in days, with median survival shown. Significances are determined by a log rank (Mantel Cox) test. **D)** % dead, CD45⁻ , non-immune ascites cells (Live/dead stain⁺, CD45⁻) from the NSG ascites fluid. **B, D)** Mean+SEM is shown and significances are determined by a Mann-Whitney t-test.

Figure 3.7: Ex vivo treatment of ID8-VEGF-Defensin cells with low dose AZA decreases viable cell number, increases apoptosis, and disrupts the cell cycle.
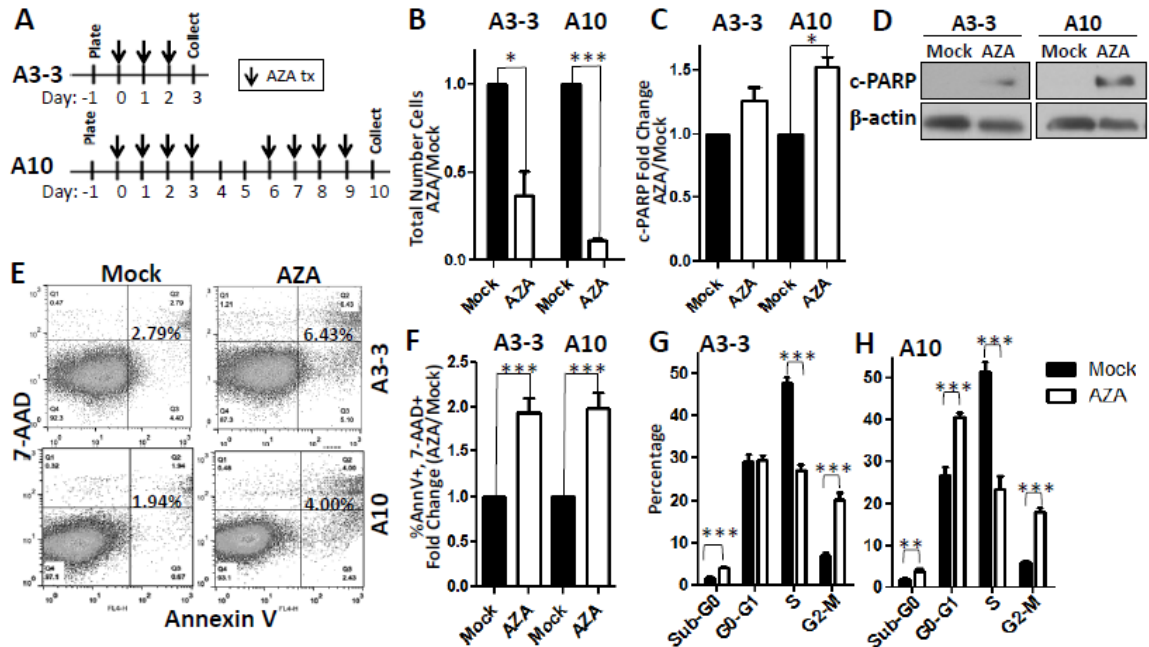
A) 3 or 10 day *in vitro* treatment with 500nM AZA . **B)** Total number of cells relative to mock. n=3. **C)** Quantification of c-PARP levels in AZA treated cells relative to Mock. n=3. **D)** A representative western blot of c-PARP levels. **E-F)** Percentage of annexin V$^+$ and 7-AAD$^+$ apoptotic cells. Representative flow cytometry data is shown (E) along with quantification (F). n=3. **G-H)** Cell cycle analysis, determined by BrdU incorporation and 7-AAD staining of DNA content. n=3. Mean+SEM is shown, and significances are determined by Mann-Whitney t-tests.

Supplemental Table 3.1: Top Upstream transcriptional regulators in murine immune cells sorted from ascites of mice treated with AZA.

Gene	Primer Sequence (5'-3')	Accession #
mERVL gag-pol	ACATACCCAGTAATGGTCAGCAC ATTGGTTAGCCAGTACCAAAGGT	2065208
mErv3*	CATAGCCTCTACCTTCTGTCTGGT AGAGGTCATAGCATTGTAGGGTTC	261245003
syncytin-A	GATGACATCCACTGCCACAC ATTGTCCGGCTCGAATAGG	AY849973.1
Peg11(Mart1) (Rtl1)	GAAACAATCAACTCATCCGAGAC AGAGTTCTTGGGCTGACCTTC	NM_184109.1
mMart8 (Cxx1c)	AAGGGCCGGGCCCTGCAGTG CTAGAAGTCCTCATCCTCCTCCCACCCG	115270961
IAP-MIA14 LTR*	Gacacgtcctaggcgaaatataac Tattgcttacatcttcaggagcaag	M17551.1
IAP-MIA14 gag*	GATCAATTAGCGGAGGTCTCTAG CCAGTCTGTTTCTTCAGAGGAGAA	M17551.1
IAPEZ gag*	Gctctccctagtatgggcaaatat Aatctctctgctctggagtcaaag	AC003993
mMTV7/8/9*	CTACACTTAGGAGAGAAGCAGC ATGTCTTTGTCTGATGGGCTCAT	M90535.1, X05400.1, M29600.1
B1* (consensus)	GAGGCAGAGGCAGGCGGATT GTTTCTCTGTGTAGCCCTGGC	Munclinger et al.2003
mGapdh	AGAAACCTGCCAAGTATGATGAC AGACAACCTGGTCCTCAGTGT	126012538
mouse ß-actin	TTCTTGGGTATGGAATCCTGTGG TGGCATAGAGGTCTTTACGGATG	145966868
mouse 18SrRNA	ATGGCCGTTCTTAGTTGGTG GAACGCCACTTGTCCCTCTA	120444899

Mouse E16.5 placenta was used as a positive internal control: *= semi-qPCR, all other genes were done with full qPCR according to Henke et al. 2013 Differentiation and Henke et al. 2015, Retrovirology.

Supplemental Table 3.2: Top upstream transcriptional regulators in murine immune cells sorted from ascites of mice treated with AZA (Supplemental Figure 4.5A).

CD8+	CD4+	CD11b+
Ifnb1	Trim24	Trim24
Trp53	Trp53	Irf7
Alkbh5	Alkbh5	Ifn alpha/beta
Dysf	Fzd9	Irf3
Ptger2	Irf7	Ptger4
Ptger4	Ifnar	Ifnar
Irgm1	Irf3	IL12
Ifng	Dnase2a	Stat1
Irf3	Stat2	Nr3c1
Irf7	Tcf7l2	Ddx58

Ingenuity pathway analysis identified type I interferon pathway associated genes as top upstream regulators of the transcriptional program in AZA treated CD4+, CD8+, and CD11b+cells.

Supplemental Figure 3.1:
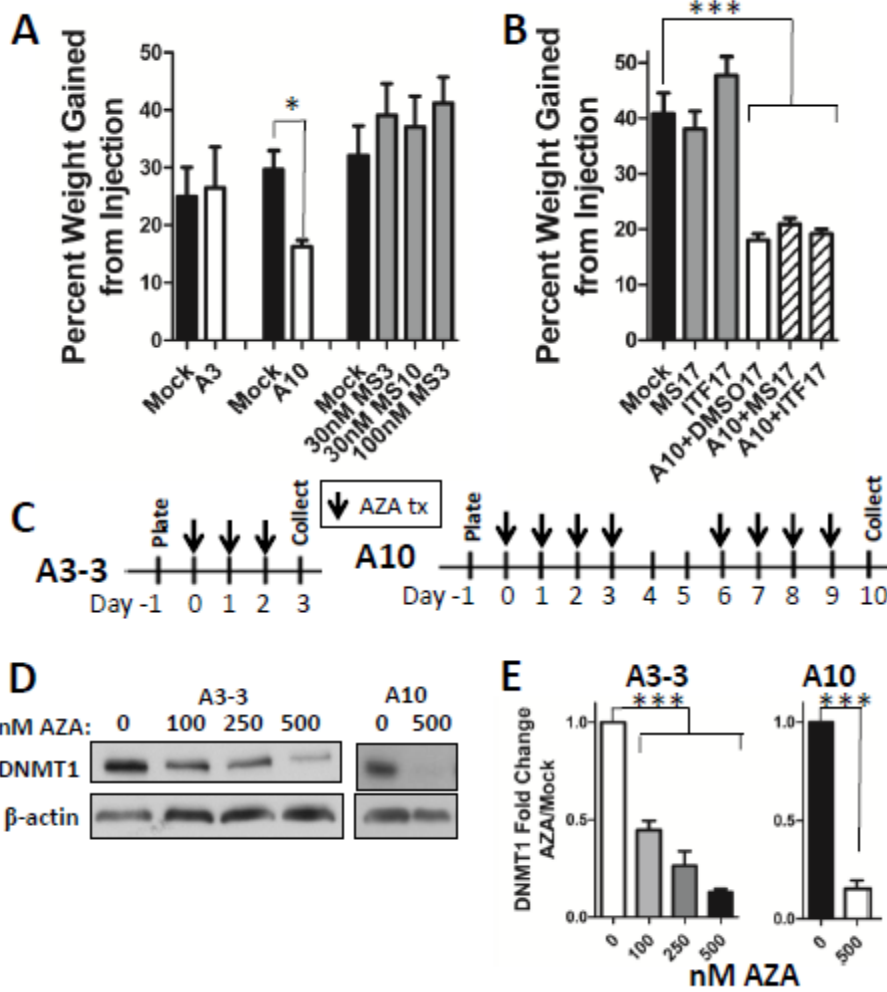
A, B) Percent weight gained by the mice in Figure 3.1B, C. **C)**Treatment schematic for collection of cells treated with 500nM AZA (A) at day 3 (A3) or day 10 (A10). **D)** Representative Western blot of DNMT1 levels at day 3 or 10. **E)** Quantification of DNMT1 western blots. n=3.

Supplemental Figure 3.2:
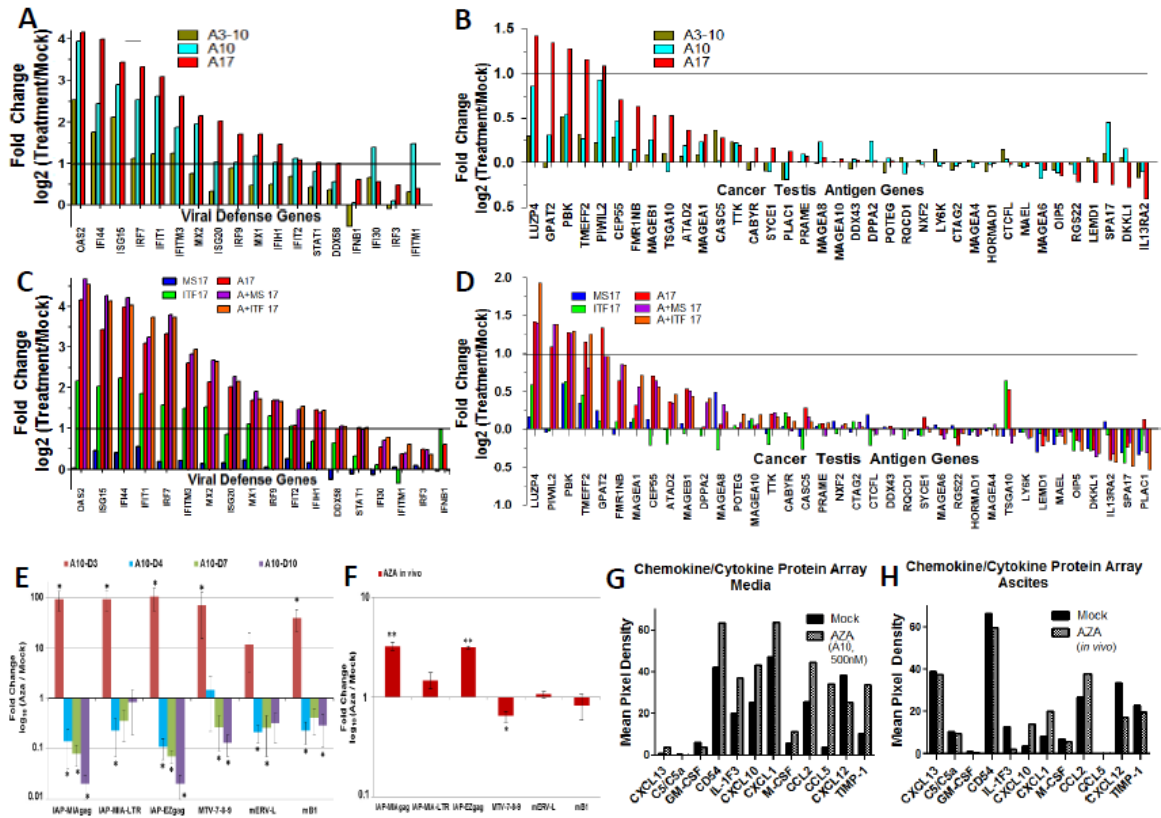
A-D) ID8-Vegf-Defensincells were treated withA3-10, A10, A17, HDACi17, A+HDACi17as shown in Figure 3.1A. Expression of viral defense genes (A,C), and expression of cancer testis antigen genes (B,D) are shown. The horizontal line at log2 fold change=1 indicate a 2 fold increase in expression. **E-F)** Mean fold increase of mERVand B1 gene expression levels compared to Mock treated; (qPCR) at days 3, 4, 7, and 10 of an A10 treatment schedule (n=3); mean +/-sem; *=P<0.05. **G-H)** Protein levels of chemokinesand cytokines assessed using the Proteome Profiles Mouse Cytokine Array Kit from R&D systems (n=1). **G)** Cells were treated with schedule A10, and media was collected. **H)** Ascites from Mock or AZA treated mice were collected at week 4.5 after injection of tumor cells (Supplemental Figure 3.6).

Supplemental Figure 3.3:
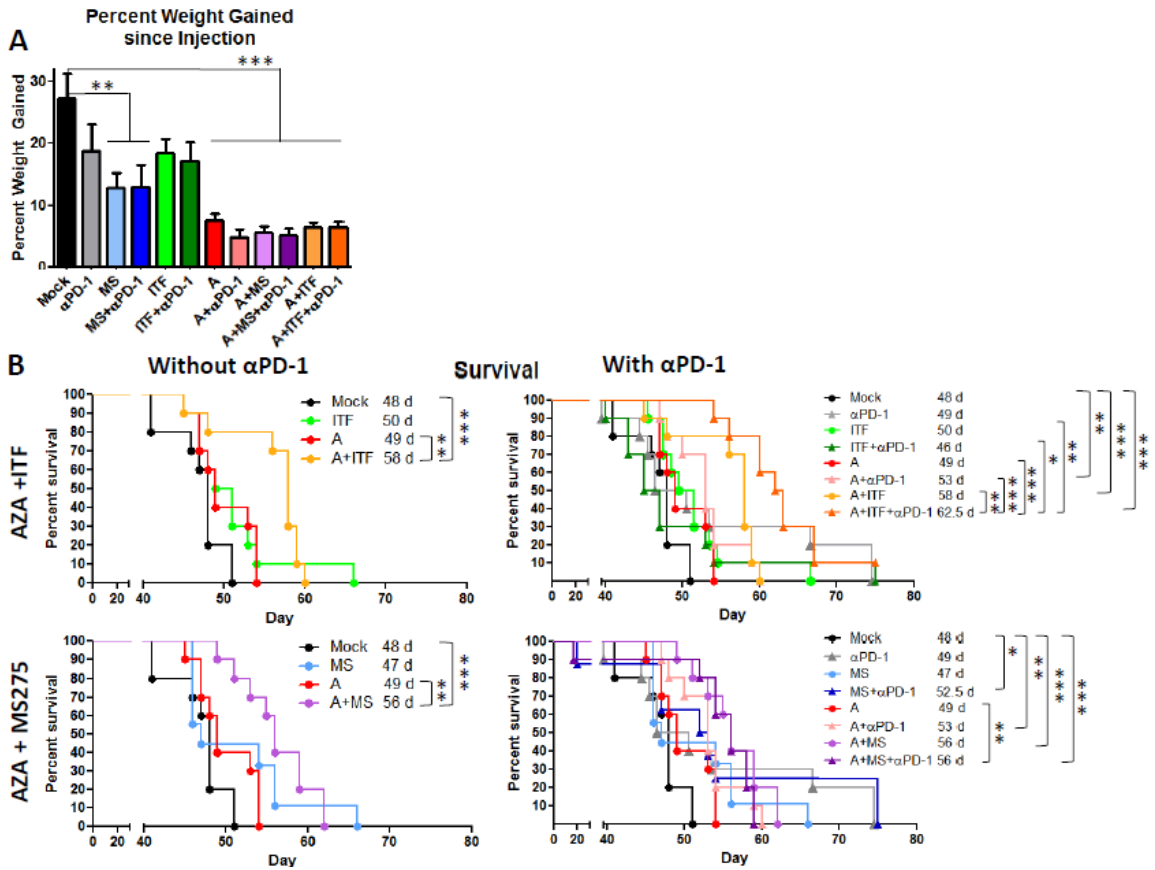
Mice were treated as described in Figure 3.3 (n=1). **A)** Percentage weight gained by the mice in Figure 3.3 at week 5 mimics ascites volume. **B)** Survival data for all 12 arms of the experiment.

Supplemental Figure 3.4
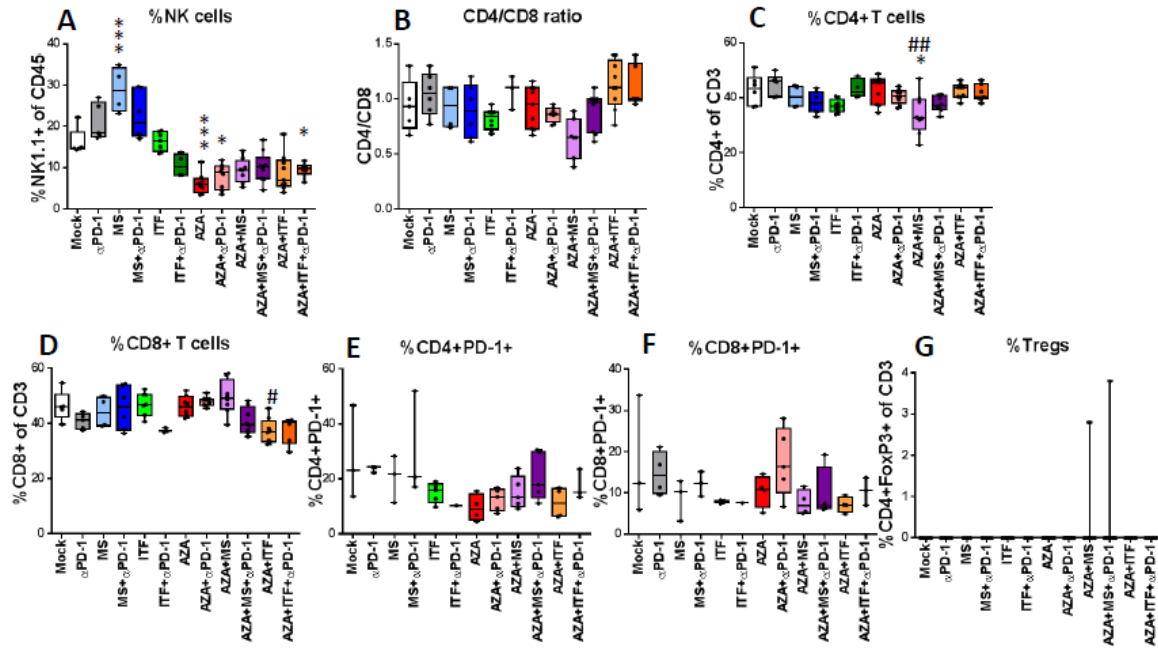
Ascites fluid was drained from the mice in Figure 3.3 at week 6.5, and cells were analyzed via FACS. **A)** % NK cells (NK1.1+) of CD45+cells; **B)** CD4+/CD8+cell ratio; **C)** %CD4+of all T cells; **D)** %CD8+of all T cells; **E)** %CD4+PD1+T cells of CD4+ T cells; **F)** %CD8+PD1+T cells of CD8+ T cells; **G)**%T regulatory cells (CD4+, FoxP3+) of all CD3+T cells. n=1.

Supplemental Figure 3.5:
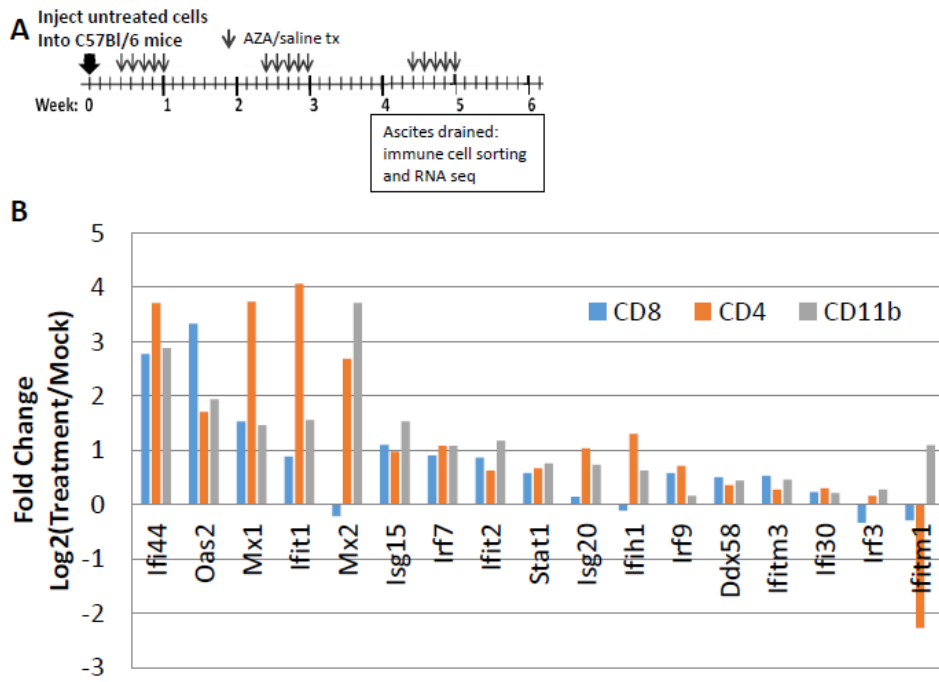
RNA sequencing of sorted immune cell populations from ascites fluid showed up-regulation of viral defense genes upon AZA treatment in tumor bearing mice.

A) Treatment schematic. **B)** Viral defense gene expression.

Supplemental Figure 3.6:
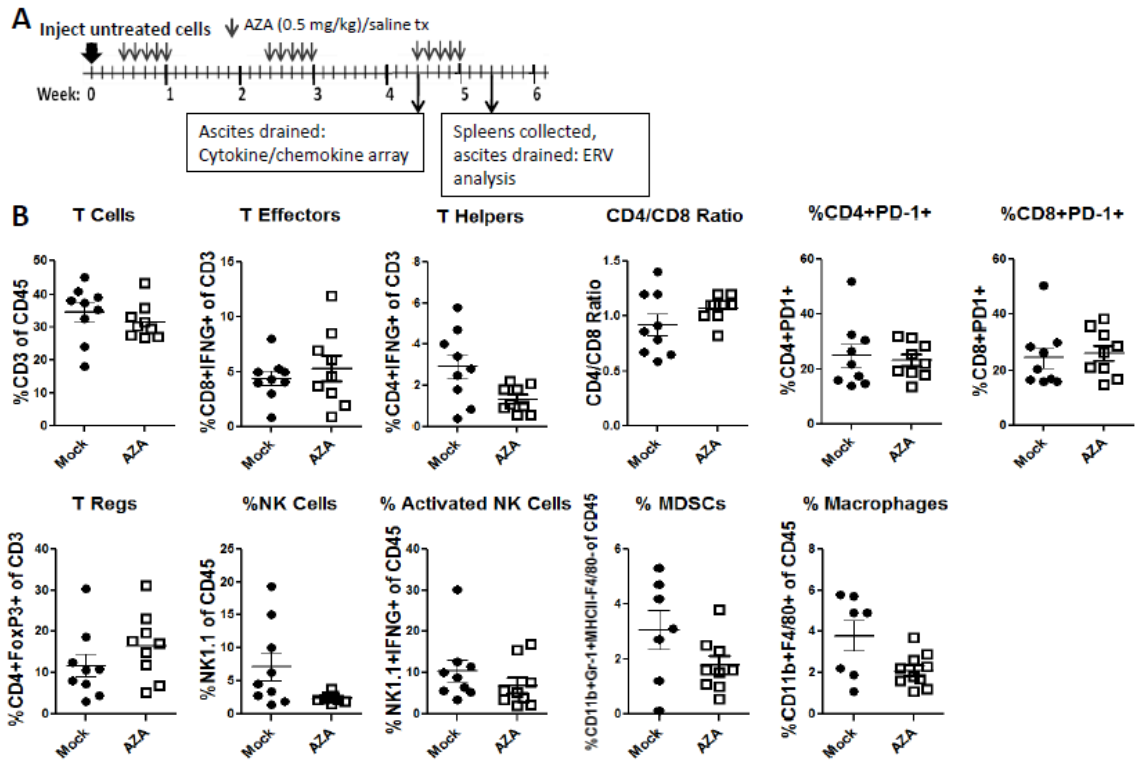
A) Treatment schematic for mice treated only with Mock or AZA.2.5x106cells were injected i.p. into 8-10 week old female C57Bl/6 mice and treated on the days indicated with an arrow in the schematic (the same schedule as Figure 3.3).**B)** Spleens were collected from Mock or AZA treated tumor bearing mice at week 5.5. Spleens were filtered and washed to a single cell suspension, and the cells were analyzed via FACS. n=1.

Chapter 4: Conclusions and Future Directions

Conclusions and Future Directions

In this study, we have used a syngeneic mouse model of ovarian cancer to show that combination epigenetic therapy can sensitize ovarian tumors to immune checkpoint blockade (α-PD-1). The demethylating agent, AZA, has direct effects on the tumor cells themselves that include induction of immune gene signaling, apoptosis, and cell cycle arrest. Perhaps because of these changes, when AZA treated tumor cells are injected into mice, there is an increase in the number of CD45$^+$ cells in the tumor microenvironment, a decrease in tumor burden and an increase in survival of the mice. Interestingly, when a histone deacetylase inhibitor is used as a single agent to treat the tumor cells, the above parameters do not change significantly, and when an HDACi is added to AZA in the pretreatment model or in an immunodeficient mouse, it does not enhance the effect of AZA for the most part. This is in contrast to when the tumor and intact immune system are both treated *in vivo* with AZA and an HDACi. In that case, the combination therapy significantly extends survival in the mice over that of AZA alone, and decreases tumor burden compared to the single agents. Unsurprisingly, treatment *in vivo* causes more changes in the immune microenvironment than pretreatment of the tumor cells. AZA *in vivo* treatment causes small but significant increases in the activation of CD8$^+$ and CD4$^+$ T cells and NK cells, as well as a decrease in the percentage of macrophages. The addition of an HDACi significantly enhances these effects, and importantly, the combination of AZA and the HDACi Givinostat improved the response of the tumor to anti-PD-1 therapy. The induction of the type I interferon response by AZA may be responsible for many of these effects. When the interferon-α,β receptor 1 (IFNAR1) is blocked *in vivo*, the AZA driven decrease in ascites burden and increase in survival are both lost. Furthermore, α-IFNAR1 blocks the increase in the number of CD45$^+$ cells per mL, and the increase in the percentage of activated CD8$^+$ T cells and NK cells.

For this study, we used a model of ovarian cancer derived from ovarian surface epithelial cells (131-134). In some potentially important ways, these cells have key differences from human serous ovarian cancer. For example, a recent paper revealed that the ID8 model does not have functional mutations in genes that are characteristic of high grade serous ovarian carcinoma, including Trp53, Brca1, Brca2, Nf1, or Rb1 (144). Also, homologous recombination remained intact in the cells, while there are homologous recombination defects in 50% of high grade serous carcinomas (144). In this study, the authors used CRISPR/Cas9 technology to generate either Trp53$^{-/-}$ or Trp53$^{-/-}$Brca$^{-/-}$ ID8 cells, and the loss of p53 triggered an increase in suppressive myeloid populations in the tumor microenvironment. Our lab acquired these cells, and it will be especially important to determine if p53 status affects their response to epigenetic therapy, especially in terms of the immune microenvironment. In a model with more immune suppressive myeloid cells at baseline, we will need to establish whether the AZA effect of decreasing macrophages and MDSCs in the ascites fluid is maintained. If so, it is possible that AZA could be even more effective in a model that is more immunosuppressed at baseline, by relieving that suppression, or AZA may not lower the myeloid cells enough to have an effect on tumor burden, or perhaps decreases in myeloid cells are not the sole factor in regulating the response. In the second case, combination epigenetic therapy could be more effective and essential.   It will be important to answer these questions in a model that is more relevant to human disease.

In our current ID8 model, we have already established that AZA can induce the expression of immune related genes *in vitro*, including CTAs, chemokines, cytokines, and viral defense gene, in a similar manner to the effect we observed in human ovarian cancer cell lines. Furthermore, we have shown that AZA also can cause the upregulation of endogenous retroviruses and chemokines and cytokines both *in vitro* and *in vivo*. In the future, we plan to use cells sorted from the ascites fluid of treated mice to

establish that AZA also upregulates other interferon stimulated genes *in vivo.* Because of the established induction of ERV transcripts *in vivo*, it is likely that immune genes are also upregulated. Furthermore, additional studies could be done on establishing the effects of epigenetic agents administered *in vivo o*n the gene expression in immune cells. We have shown that interferon related genes are upregulated by AZA in CD8$^+$ and CD4$^+$ T cells, as well as CD11b$^+$ myeloid cells. However, some of the most striking changes in immune cell activation are with the combination of AZA and an HDACi, or the triple combination with α-PD-1. Therefore, it would be useful to study the effects of combination therapy on the gene expression profiles of the immune cells, in addition to the tumor cells. Because immune gene signaling in the tumor is not significantly enhanced by the addition of an HDACi to AZA, but there are significant increases in the activation of CD8$^+$, CD4$^+$ and NK cells, there may be interesting differences in the gene expression changes in the immune cells. If so, taken with the fact that the combination is not more effective than AZA alone in tumor pretreatment or NSG models, this would suggest that changes induced in the immune cells are an important factor in the effects of the combination epigenetic therapy.

   In addition to collecting more data on the gene expression changes caused by the epigenetic drugs, there are several experiments that can further elucidate which components of the model are critical for the reduction in tumor burden. First, pre-treatment of the tumor cells and then injecting them into NSG mice could help answer the question of whether the changes in the pre-treated tumor cells that lead to tumor reduction in the C57Bl/6 mice are tumor intrinsic or immune related. In the pre-treatment experiments conducted with C57Bl/6 mice, the effects on the tumor cells after a 10 day treatment in culture that lead to tumor reduction could be mediated through mechanisms of apoptosis and cell cycle arrest, or through the recruitment of immune cells and tumor cell killing through immune mechanisms. There is an AZA anti-tumorigenic effect *in vivo*

in NSG mice, suggesting that with longer term treatment the apoptosis and cell cycle effects are more dominant than the effects from immune cell tumor killing. However, with a 10 day pretreatment followed by no treatment *in vivo*, it may be that the upregulation of immune gene pathways is more important, and we may not see an AZA effect with pretreated tumor cells in the NSG mice.

A second way to elucidate which, if any, immune mechanisms are important for the reduction of tumor burden with AZA would be use antibodies to deplete CD8$^+$ T cells and/or NK cells. By blocking IFNAR1, we have shown that inhibiting the interferon response rescued the increase in activated NK cells and CD8$^+$ T cells in AZA treated immunocompetent mice, and also rescued the decrease in ascites burden. However, it is possible that the main reason that ascites burden was rescued was because of the blockage of interferon induced apoptosis of the tumor cells. One way to prove that the reduction of activated CD8$^+$ and NK cells caused the rescue of the ascites burden would be to use antibodies blocking the activity of those cells, but not the entire interferon response. If blocking only the activated immune cells rescues the decrease in tumor burden, then the interferon response-related recruitment and activation of those cells is most likely responsible for the antitumorigenic effect. However, if the blockage of those cells does not rescue the ascites burden decrease, then it is most likely an interferon induced apoptotic effect that causes the decrease in tumor burden.

Finally, to be thorough, we should perform the α-IFNAR1 blocking experiment in the NSG mice to establish that the AZA antitumorigenic effect is also rescued without a complete immune system present. If the interferon induced apoptosis is being rescued, we would expect to see a rescue of the ascites burden in the NSG mice, as well as the C57Bl/6. Because we saw a complete rescue of the response in the C57Bl/6 mice, it would imply that both apoptotic and immune mechanisms of reducing tumor burden are being rescued. Therefore, it is likely that the α-IFNAR1 would also rescue the AZA

response in the NSG mice. Antibody depletion experiments targeting tumor cell killing

immune cells would be more revealing, because the immune response (which would be

blocked) would be isolated from the apoptotic effects of the interferon response (which

would still be present in the immunocompetent mice), and therefore is more informative

about which downstream parts of the interferon response are important to the AZA

antitumorigenic effect.

In addition to further elucidating which components of the interferon response are

responsible for the anti-tumorigenic effect of AZA, it will be important to determine if α-

IFNAR1 rescues the effects of the combination epigenetic therapy- specifically the

enhanced activation of immune cells and the sensitization to α-PD-1. Because the

HDACi did not increase the expression of the anti-viral genes in tumor cells *in vitro* when

added to AZA, it may seem like the interferon response in the tumor cells is not the

driving force of the combination effects. However, the combination did increase the

percentage of activated immune cells, and decrease the percentage of macrophages.

This may be due to effects on the immune cells themselves, since the combination

therapy did not provide a benefit in the NSG mice. Notably, these HDACi effects

required AZA, as the HDACi as single agents did not affect tumor burden or most of the

immune parameters in any of the models. Therefore, the implication is that AZA *in vivo*

treatment is required before the HDACi can have an effect on the immune cells. It may

well be that when the AZA induced interferon signaling is blocked, the HDACi

combination is not effective at further reducing tumor burden or activating immune cells.

Potentially, the recruitment and low level activation of the immune cells by AZA, which is

dependent on the interferon response, is necessary for the additional benefits of the

combination therapy. Additional information is needed, such as the baseline induction of

interferon stimulated genes in immune cells by combination therapy, discussed above,

and whether any potential induction of those genes by the combination is rescued by α-

IFNAR1. Blocking anti-IFNAR1 in the combination treated immunocompetent mice would be informative, as we would first learn whether the efficacy of the combination therapy and its sensitization effect are interferon related at all, and also would learn if interferon mediated gene expression changes are taking place in the tumor or the immune cells.

Understanding the mechanism by which combination therapy can sensitize tumors to immune checkpoint blockade is a crucial step to improving clinical trial design and outcomes for patients. Melanoma patients have already been shown to have an improved response to immune checkpoint blockade (α-CTLA-4) with a higher viral defense signature (118). If it is shown that the interferon response is necessary for epigenetic combination therapy and sensitization, this could indicate that patients with low interferon signaling could benefit from not just AZA, but also combination epigenetic therapy before receiving immune checkpoint blockade. As interferon gene upregulation was observed in lung cancer patients (64) and in decitabine treated ovarian cancer patients (117), it may be possible to learn from the upcoming ovarian cancer trial (178) if the AZA driven upregulation of the interferon genes in ovarian cancer patients correlates with an improvement in response to α-PD-1. Proof that combination epigenetic therapy in patients also functions through the interferon pathway to sensitize tumors could help inform the design of clinical trials so that they include an HDACi with a DNMTi to improve the response to immune checkpoint blockade.

References

1. Allis CD, Caparros M-L, Jenuwein T, Reinberg D, Lachlan M. Epigenetics. Cold Spring Harbor Laboratory Press; 2015.
2. Baylin SB, Jones PA. A decade of exploring the cancer epigenome - biological and translational implications. Nat Rev Cancer **2011**;11:726-34
3. Herman JG, Baylin SB. Gene silencing in cancer in association with promoter hypermethylation. N Engl J Med **2003**;349:2042-54
4. Jones PA, Baylin SB. The epigenomics of cancer. Cell **2007**;128:683-92
5. Bird A. DNA methylation patterns and epigenetic memory. Genes Dev **2002**;16:6-21
6. Yang X, Han H, De Carvalho DD, Lay FD, Jones PA, Liang G. Gene body methylation can alter gene expression and is a therapeutic target in cancer. Cancer Cell **2014**;26:577-90
7. Denis H, Ndlovu MN, Fuks F. Regulation of mammalian DNA methyltransferases: a route to new mechanisms. EMBO Rep **2011**;12:647-56
8. Sharif J, Muto M, Takebayashi S, Suetake I, Iwamatsu A, Endo TA, *et al.* The SRA protein Np95 mediates epigenetic inheritance by recruiting Dnmt1 to methylated DNA. Nature **2007**;450:908-12
9. Avvakumov GV, Walker JR, Xue S, Li Y, Duan S, Bronner C, *et al.* Structural basis for recognition of hemi-methylated DNA by the SRA domain of human UHRF1. Nature **2008**;455:822-5
10. Jair KW, Bachman KE, Suzuki H, Ting AH, Rhee I, Yen RW, *et al.* De novo CpG island methylation in human cancer cells. Cancer Res **2006**;66:682-92
11. Jurkowska RZ, Jurkowski TP, Jeltsch A. Structure and function of mammalian DNA methyltransferases. Chembiochem **2011**;12:206-22
12. Handa V, Jeltsch A. Profound flanking sequence preference of Dnmt3a and Dnmt3b mammalian DNA methyltransferases shape the human epigenome. J Mol Biol **2005**;348:1103-12
13. Li B, Carey M, Workman JL. The role of chromatin during transcription. Cell **2007**;128:707-19
14. Tessarz P, Kouzarides T. Histone core modifications regulating nucleosome structure and dynamics. Nat Rev Mol Cell Biol **2014**;15:703-8
15. Ropero S, Esteller M. The role of histone deacetylases (HDACs) in human cancer. Mol Oncol **2007**;1:19-25
16. Zahnow CA, Topper M, Stone M, Murray-Stewart T, Li H, Baylin SB, *et al.* Inhibitors of DNA Methylation, Histone Deacetylation, and Histone Demethylation: A Perfect Combination for Cancer Therapy. Adv Cancer Res **2016**;130:55-111
17. Bantscheff M, Hopf C, Savitski MM, Dittmann A, Grandi P, Michon AM, *et al.* Chemoproteomics profiling of HDAC inhibitors reveals selective targeting of HDAC complexes. Nat Biotechnol **2011**;29:255-65
18. Ellis L, Atadja PW, Johnstone RW. Epigenetics in cancer: targeting chromatin modifications. Mol Cancer Ther **2009**;8:1409-20
19. Wang GG, Allis CD, Chi P. Chromatin remodeling and cancer, Part I: Covalent histone modifications. Trends Mol Med **2007**;13:363-72
20. Herman JG, Latif F, Weng Y, Lerman MI, Zbar B, Liu S, *et al.* Silencing of the VHL tumor-suppressor gene by DNA methylation in renal carcinoma. Proc Natl Acad Sci U S A **1994**;91:9700-4
21. Jones PA, Baylin SB. The fundamental role of epigenetic events in cancer. Nat Rev Genet **2002**;3:415-28

22. Hansen KD, Timp W, Bravo HC, Sabunciyan S, Langmead B, McDonald OG*, et al.* Increased methylation variation in epigenetic domains across cancer types. Nat Genet **2011**;43:768-75

23. Azad N, Zahnow CA, Rudin CM, Baylin SB. The future of epigenetic therapy in solid tumours--lessons from the past. Nat Rev Clin Oncol **2013**;10:256-66

24. Stresemann C, Brueckner B, Musch T, Stopper H, Lyko F. Functional diversity of DNA methyltransferase inhibitors in human cancer cell lines. Cancer Res **2006**;66:2794-800

25. Stresemann C, Lyko F. Modes of action of the DNA methyltransferase inhibitors azacytidine and decitabine. Int J Cancer **2008**;123:8-13

26. Li LH, Olin EJ, Buskirk HH, Reineke LM. Cytotoxicity and mode of action of 5-azacytidine on L1210 leukemia. Cancer Res **1970**;30:2760-9

27. Cihak A. Biological effects of 5-azacytidine in eukaryotes. Oncology **1974**;30:405-22

28. Li LH, Olin EJ, Fraser TJ, Bhuyan BK. Phase specificity of 5-azacytidine against mammalian cells in tissue culture. Cancer Res **1970**;30:2770-5

29. Santi DV, Norment A, Garrett CE. Covalent bond formation between a DNA-cytosine methyltransferase and DNA containing 5-azacytosine. Proc Natl Acad Sci U S A **1984**;81:6993-7

30. Ghoshal K, Datta J, Majumder S, Bai S, Kutay H, Motiwala T*, et al.* 5-Aza-deoxycytidine induces selective degradation of DNA methyltransferase 1 by a proteasomal pathway that requires the KEN box, bromo-adjacent homology domain, and nuclear localization signal. Mol Cell Biol **2005**;25:4727-41

31. Egger G, Liang G, Aparicio A, Jones PA. Epigenetics in human disease and prospects for epigenetic therapy. Nature **2004**;429:457-63

32. Issa JP, Roboz G, Rizzieri D, Jabbour E, Stock W, O'Connell C*, et al.* Safety and tolerability of guadecitabine (SGI-110) in patients with myelodysplastic syndrome and acute myeloid leukaemia: a multicentre, randomised, dose-escalation phase 1 study. Lancet Oncol **2015**;16:1099-110

33. Newbold A, Falkenberg KJ, Prince HM, Johnstone RW. How do tumor cells respond to HDAC inhibition? FEBS J **2016**;283:4032-46

34. Bradner JE, West N, Grachan ML, Greenberg EF, Haggarty SJ, Warnow T*, et al.* Chemical phylogenetics of histone deacetylases. Nat Chem Biol **2010**;6:238-43

35. Yardley DA, Ismail-Khan RR, Melichar B, Lichinitser M, Munster PN, Klein PM*, et al.* Randomized phase II, double-blind, placebo-controlled study of exemestane with or without entinostat in postmenopausal women with locally recurrent or metastatic estrogen receptor-positive breast cancer progressing on treatment with a nonsteroidal aromatase inhibitor. J Clin Oncol **2013**;31:2128-35

36. Juergens RA, Wrangle J, Vendetti FP, Murphy SC, Zhao M, Coleman B*, et al.* Combination epigenetic therapy has efficacy in patients with refractory advanced non-small cell lung cancer. Cancer Discov **2011**;1:598-607

37. Galli M, Salmoiraghi S, Golay J, Gozzini A, Crippa C, Pescosta N*, et al.* A phase II multiple dose clinical trial of histone deacetylase inhibitor ITF2357 in patients with relapsed or progressive multiple myeloma. Ann Hematol **2010**;89:185-90

38. Bachman KE, Rountree MR, Baylin SB. Dnmt3a and Dnmt3b are transcriptional repressors that exhibit unique localization properties to heterochromatin. J Biol Chem **2001**;276:32282-7

39. Fuks F, Burgers WA, Brehm A, Hughes-Davies L, Kouzarides T. DNA methyltransferase Dnmt1 associates with histone deacetylase activity. Nat Genet **2000**;24:88-91

40.   Ling Y, Sankpal UT, Robertson AK, McNally JG, Karpova T, Robertson KD. Modification of de novo DNA methyltransferase 3a (Dnmt3a) by SUMO-1 modulates its interaction with histone deacetylases (HDACs) and its capacity to repress transcription. Nucleic Acids Res **2004**;32:598-610

41.   Robertson KD, Ait-Si-Ali S, Yokochi T, Wade PA, Jones PL, Wolffe AP. DNMT1 forms a complex with Rb, E2F1 and HDAC1 and represses transcription from E2F-responsive promoters. Nat Genet **2000**;25:338-42

42.   Rountree MR, Bachman KE, Baylin SB. DNMT1 binds HDAC2 and a new co-repressor, DMAP1, to form a complex at replication foci. Nat Genet **2000**;25:269-77

43.   Nan X, Ng HH, Johnson CA, Laherty CD, Turner BM, Eisenman RN*, et al.* Transcriptional repression by the methyl-CpG-binding protein MeCP2 involves a histone deacetylase complex. Nature **1998**;393:386-9

44.   Parry L, Clarke AR. The Roles of the Methyl-CpG Binding Proteins in Cancer. Genes Cancer **2011**;2:618-30

45.   Denslow SA, Wade PA. The human Mi-2/NuRD complex and gene regulation. Oncogene **2007**;26:5433-8

46.   Ebert DH, Gabel HW, Robinson ND, Kastan NR, Hu LS, Cohen S*, et al.* Activity-dependent phosphorylation of MeCP2 threonine 308 regulates interaction with NCoR. Nature **2013**;499:341-5

47.   Zhang Y, Ng HH, Erdjument-Bromage H, Tempst P, Bird A, Reinberg D. Analysis of the NuRD subunits reveals a histone deacetylase core complex and a connection with DNA methylation. Genes Dev **1999**;13:1924-35

48.   Cai Y, Geutjes EJ, de Lint K, Roepman P, Bruurs L, Yu LR*, et al.* The NuRD complex cooperates with DNMTs to maintain silencing of key colorectal tumor suppressor genes. Oncogene **2014**;33:2157-68

49.   Wong MM, Guo C, Zhang J. Nuclear receptor corepressor complexes in cancer: mechanism, function and regulation. Am J Clin Exp Urol **2014**;2:169-87

50.   Ahuja N, Easwaran H, Baylin SB. Harnessing the potential of epigenetic therapy to target solid tumors. J Clin Invest **2014**;124:56-63

51.   Cameron EE, Bachman KE, Myohanen S, Herman JG, Baylin SB. Synergy of demethylation and histone deacetylase inhibition in the re-expression of genes silenced in cancer. Nat Genet **1999**;21:103-7

52.   Antequera F, Macleod D, Bird AP. Specific protection of methylated CpGs in mammalian nuclei. Cell **1989**;58:509-17

53.   Eden S, Hashimshony T, Keshet I, Cedar H, Thorne AW. DNA methylation models histone acetylation. Nature **1998**;394:842

54.   Zhu WG, Lakshmanan RR, Beal MD, Otterson GA. DNA methyltransferase inhibition enhances apoptosis induced by histone deacetylase inhibitors. Cancer Res **2001**;61:1327-33

55.   Steele N, Finn P, Brown R, Plumb JA. Combined inhibition of DNA methylation and histone acetylation enhances gene re-expression and drug sensitivity in vivo. Br J Cancer **2009**;100:758-63

56.   Chen MY, Liao WS, Lu Z, Bornmann WG, Hennessey V, Washington MN*, et al.* Decitabine and suberoylanilide hydroxamic acid (SAHA) inhibit growth of ovarian cancer cell lines and xenografts while inducing expression of imprinted tumor suppressor genes, apoptosis, G2/M arrest, and autophagy. Cancer **2011**;117:4424-38

57.   Venturelli S, Armeanu S, Pathil A, Hsieh CJ, Weiss TS, Vonthein R, *et al.* Epigenetic combination therapy as a tumor-selective treatment approach for hepatocellular carcinoma. Cancer **2007**;109:2132-41

58.   Belinsky SA, Klinge DM, Stidley CA, Issa JP, Herman JG, March TH, *et al.* Inhibition of DNA methylation and histone deacetylation prevents murine lung cancer. Cancer Res **2003**;63:7089-93

59.   Tellez CS, Grimes MJ, Picchi MA, Liu Y, March TH, Reed MD, *et al.* SGI-110 and entinostat therapy reduces lung tumor burden and reprograms the epigenome. Int J Cancer **2014**;135:2223-31

60.   Ecke I, Petry F, Rosenberger A, Tauber S, Monkemeyer S, Hess I, *et al.* Antitumor effects of a combined 5-aza-2'deoxycytidine and valproic acid treatment on rhabdomyosarcoma and medulloblastoma in Ptch mutant mice. Cancer Res **2009**;69:887-95

61.   Braiteh F, Soriano AO, Garcia-Manero G, Hong D, Johnson MM, Silva Lde P, *et al.* Phase I study of epigenetic modulation with 5-azacytidine and valproic acid in patients with advanced cancers. Clin Cancer Res **2008**;14:6296-301

62.   Stathis A, Hotte SJ, Chen EX, Hirte HW, Oza AM, Moretto P, *et al.* Phase I study of decitabine in combination with vorinostat in patients with advanced solid tumors and non-Hodgkin's lymphomas. Clin Cancer Res **2011**;17:1582-90

63.   Chu BF, Karpenko MJ, Liu Z, Aimiuwu J, Villalona-Calero MA, Chan KK, *et al.* Phase I study of 5-aza-2'-deoxycytidine in combination with valproic acid in non-small-cell lung cancer. Cancer Chemother Pharmacol **2013**;71:115-21

64.   Wrangle J, Wang W, Koch A, Easwaran H, Mohammad HP, Vendetti F, *et al.* Alterations of immune response of Non-Small Cell Lung Cancer with Azacytidine. Oncotarget **2013**;4:2067-79

65.   Pardoll DM. The blockade of immune checkpoints in cancer immunotherapy. Nat Rev Cancer **2012**;12:252-64

66.   Tivol EA, Borriello F, Schweitzer AN, Lynch WP, Bluestone JA, Sharpe AH. Loss of CTLA-4 leads to massive lymphoproliferation and fatal multiorgan tissue destruction, revealing a critical negative regulatory role of CTLA-4. Immunity **1995**;3:541-7

67.   Freeman GJ, Long AJ, Iwai Y, Bourque K, Chernova T, Nishimura H, *et al.* Engagement of the PD-1 immunoinhibitory receptor by a novel B7 family member leads to negative regulation of lymphocyte activation. J Exp Med **2000**;192:1027-34

68.   Nishimura H, Nose M, Hiai H, Minato N, Honjo T. Development of lupus-like autoimmune diseases by disruption of the PD-1 gene encoding an ITIM motif-carrying immunoreceptor. Immunity **1999**;11:141-51

69.   Dong H, Strome SE, Salomao DR, Tamura H, Hirano F, Flies DB, *et al.* Tumor-associated B7-H1 promotes T-cell apoptosis: a potential mechanism of immune evasion. Nat Med **2002**;8:793-800

70.   Ishida Y, Agata Y, Shibahara K, Honjo T. Induced expression of PD-1, a novel member of the immunoglobulin gene superfamily, upon programmed cell death. EMBO J **1992**;11:3887-95

71.   Barber DL, Wherry EJ, Masopust D, Zhu B, Allison JP, Sharpe AH, *et al.* Restoring function in exhausted CD8 T cells during chronic viral infection. Nature **2006**;439:682-7

72.   Terme M, Ullrich E, Aymeric L, Meinhardt K, Desbois M, Delahaye N, *et al.* IL-18 induces PD-1-dependent immunosuppression in cancer. Cancer Res **2011**;71:5393-9

73. Fanoni D, Tavecchio S, Recalcati S, Balice Y, Venegoni L, Fiorani R*, et al.* New monoclonal antibodies against B-cell antigens: possible new strategies for diagnosis of primary cutaneous B-cell lymphomas. Immunol Lett **2011**;134:157-60

74. Lenschow DJ, Walunas TL, Bluestone JA. CD28/B7 system of T cell costimulation. Annu Rev Immunol **1996**;14:233-58

75. Topalian SL, Drake CG, Pardoll DM. Immune checkpoint blockade: a common denominator approach to cancer therapy. Cancer Cell **2015**;27:450-61

76. Brahmer JR, Tykodi SS, Chow LQ, Hwu WJ, Topalian SL, Hwu P*, et al.* Safety and activity of anti-PD-L1 antibody in patients with advanced cancer. N Engl J Med **2012**;366:2455-65

77. Brahmer JR, Drake CG, Wollner I, Powderly JD, Picus J, Sharfman WH*, et al.* Phase I study of single-agent anti-programmed death-1 (MDX-1106) in refractory solid tumors: safety, clinical activity, pharmacodynamics, and immunologic correlates. J Clin Oncol **2010**;28:3167-75

78. Berger R, Rotem-Yehudar R, Slama G, Landes S, Kneller A, Leiba M*, et al.* Phase I safety and pharmacokinetic study of CT-011, a humanized antibody interacting with PD-1, in patients with advanced hematologic malignancies. Clin Cancer Res **2008**;14:3044-51

79. Robert C, Long GV, Brady B, Dutriaux C, Maio M, Mortier L*, et al.* Nivolumab in previously untreated melanoma without BRAF mutation. N Engl J Med **2015**;372:320-30

80. Hamid O, Robert C, Daud A, Hodi FS, Hwu WJ, Kefford R*, et al.* Safety and tumor responses with lambrolizumab (anti-PD-1) in melanoma. N Engl J Med **2013**;369:134-44

81. Motzer RJ, Rini BI, McDermott DF, Redman BG, Kuzel TM, Harrison MR*, et al.* Nivolumab for Metastatic Renal Cell Carcinoma: Results of a Randomized Phase II Trial. J Clin Oncol **2015**;33:1430-7

82. Topalian SL, Sznol M, McDermott DF, Kluger HM, Carvajal RD, Sharfman WH*, et al.* Survival, durable tumor remission, and long-term safety in patients with advanced melanoma receiving nivolumab. J Clin Oncol **2014**;32:1020-30

83. Sharma P, Allison JP. Immune checkpoint targeting in cancer therapy: toward combination strategies with curative potential. Cell **2015**;161:205-14

84. Weber JS, D'Angelo SP, Minor D, Hodi FS, Gutzmer R, Neyns B*, et al.* Nivolumab versus chemotherapy in patients with advanced melanoma who progressed after anti-CTLA-4 treatment (CheckMate 037): a randomised, controlled, open-label, phase 3 trial. Lancet Oncol **2015**;16:375-84

85. Wolchok JD, Kluger H, Callahan MK, Postow MA, Rizvi NA, Lesokhin AM*, et al.* Nivolumab plus ipilimumab in advanced melanoma. N Engl J Med **2013**;369:122-33

86. Frederick DT, Piris A, Cogdill AP, Cooper ZA, Lezcano C, Ferrone CR*, et al.* BRAF inhibition is associated with enhanced melanoma antigen expression and a more favorable tumor microenvironment in patients with metastatic melanoma. Clin Cancer Res **2013**;19:1225-31

87. Li H, Chiappinelli KB, Guzzetta AA, Easwaran H, Yen RW, Vatapalli R*, et al.* Immune regulation by low doses of the DNA methyltransferase inhibitor 5-azacitidine in common human epithelial cancers. Oncotarget **2014**;5:587-98

88. James SR, Link PA, Karpf AR. Epigenetic regulation of X-linked cancer/germline antigen genes by DNMT1 and DNMT3b. Oncogene **2006**;25:6975-85

89. Karpf AR. A potential role for epigenetic modulatory drugs in the enhancement of cancer/germ-line antigen vaccine efficacy. Epigenetics **2006**;1:116-20

90. Karpf AR, Lasek AW, Ririe TO, Hanks AN, Grossman D, Jones DA. Limited gene activation in tumor and normal epithelial cells treated with the DNA methyltransferase inhibitor 5-aza-2'-deoxycytidine. Mol Pharmacol **2004**;65:18-27

91. Woloszynska-Read A, Zhang W, Yu J, Link PA, Mhawech-Fauceglia P, Collamat G*, et al.* Coordinated cancer germline antigen promoter and global DNA hypomethylation in ovarian cancer: association with the BORIS/CTCF expression ratio and advanced stage. Clin Cancer Res **2011**;17:2170-80

92. Srivastava P, Paluch BE, Matsuzaki J, James SR, Collamat-Lai G, Taverna P*, et al.* Immunomodulatory action of the DNA methyltransferase inhibitor SGI-110 in epithelial ovarian cancer cells and xenografts. Epigenetics **2015**;10:237-46

93. Odunsi K, Matsuzaki J, James SR, Mhawech-Fauceglia P, Tsuji T, Miller A*, et al.* Epigenetic potentiation of NY-ESO-1 vaccine therapy in human ovarian cancer. Cancer Immunol Res **2014**;2:37-49

94. Leclercq S, Gueugnon F, Boutin B, Guillot F, Blanquart C, Rogel A*, et al.* A 5-aza-2'-deoxycytidine/valproate combination induces cytotoxic T-cell response against mesothelioma. Eur Respir J **2011**;38:1105-16

95. Yang D, Torres CM, Bardhan K, Zimmerman M, McGaha TL, Liu K. Decitabine and vorinostat cooperate to sensitize colon carcinoma cells to Fas ligand-induced apoptosis in vitro and tumor suppression in vivo. J Immunol **2012**;188:4441-9

96. Wang L, Amoozgar Z, Huang J, Saleh MH, Xing D, Orsulic S*, et al.* Decitabine Enhances Lymphocyte Migration and Function and Synergizes with CTLA-4 Blockade in a Murine Ovarian Cancer Model. Cancer Immunol Res **2015**;3:1030-41

97. Peng D, Kryczek I, Nagarsheth N, Zhao L, Wei S, Wang W*, et al.* Epigenetic silencing of TH1-type chemokines shapes tumour immunity and immunotherapy. Nature **2015**;527:249-53

98. Platanias LC. Mechanisms of type-I- and type-II-interferon-mediated signalling. Nat Rev Immunol **2005**;5:375-86

99. Pestka S, Langer JA, Zoon KC, Samuel CE. Interferons and their actions. Annu Rev Biochem **1987**;56:727-77

100. Pestka S, Krause CD, Walter MR. Interferons, interferon-like cytokines, and their receptors. Immunol Rev **2004**;202:8-32

101. Darnell JE, Jr., Kerr IM, Stark GR. Jak-STAT pathways and transcriptional activation in response to IFNs and other extracellular signaling proteins. Science **1994**;264:1415-21

102. Ihle JN. The Janus protein tyrosine kinase family and its role in cytokine signaling. Adv Immunol **1995**;60:1-35

103. Der SD, Zhou A, Williams BR, Silverman RH. Identification of genes differentially regulated by interferon alpha, beta, or gamma using oligonucleotide arrays. Proc Natl Acad Sci U S A **1998**;95:15623-8

104. Diamond MS, Kinder M, Matsushita H, Mashayekhi M, Dunn GP, Archambault JM*, et al.* Type I interferon is selectively required by dendritic cells for immune rejection of tumors. J Exp Med **2011**;208:1989-2003

105. Fuertes MB, Kacha AK, Kline J, Woo SR, Kranz DM, Murphy KM*, et al.* Host type I IFN signals are required for antitumor CD8+ T cell responses through CD8{alpha}+ dendritic cells. J Exp Med **2011**;208:2005-16

106. Hildner K, Edelson BT, Purtha WE, Diamond M, Matsushita H, Kohyama M*, et al.* Batf3 deficiency reveals a critical role for CD8alpha+ dendritic cells in cytotoxic T cell immunity. Science **2008**;322:1097-100

107. Aichele P, Unsoeld H, Koschella M, Schweier O, Kalinke U, Vucikuja S. CD8 T cells specific for lymphocytic choriomeningitis virus require type I IFN receptor for clonal expansion. J Immunol **2006**;176:4525-9

108. Curtsinger JM, Valenzuela JO, Agarwal P, Lins D, Mescher MF. Type I IFNs provide a third signal to CD8 T cells to stimulate clonal expansion and differentiation. J Immunol **2005**;174:4465-9

109. Hervas-Stubbs S, Riezu-Boj JI, Gonzalez I, Mancheno U, Dubrot J, Azpilicueta A*, et al.* Effects of IFN-alpha as a signal-3 cytokine on human naive and antigen-experienced CD8(+) T cells. Eur J Immunol **2010**;40:3389-402

110. Hiroishi K, Tuting T, Lotze MT. IFN-alpha-expressing tumor cells enhance generation and promote survival of tumor-specific CTLs. J Immunol **2000**;164:567-72

111. Ikeda H, Old LJ, Schreiber RD. The roles of IFN gamma in protection against tumor development and cancer immunoediting. Cytokine Growth Factor Rev **2002**;13:95-109

112. Chin YE, Kitagawa M, Kuida K, Flavell RA, Fu XY. Activation of the STAT signaling pathway can cause expression of caspase 1 and apoptosis. Mol Cell Biol **1997**;17:5328-37

113. Detjen KM, Farwig K, Welzel M, Wiedenmann B, Rosewicz S. Interferon gamma inhibits growth of human pancreatic carcinoma cells via caspase-1 dependent induction of apoptosis. Gut **2001**;49:251-62

114. Spranger S, Spaapen RM, Zha Y, Williams J, Meng Y, Ha TT*, et al.* Up-regulation of PD-L1, IDO, and T(regs) in the melanoma tumor microenvironment is driven by CD8(+) T cells. Sci Transl Med **2013**;5:200ra116

115. Taube JM, Anders RA, Young GD, Xu H, Sharma R, McMiller TL*, et al.* Colocalization of inflammatory response with B7-h1 expression in human melanocytic lesions supports an adaptive resistance mechanism of immune escape. Sci Transl Med **2012**;4:127ra37

116. Karpf AR, Peterson PW, Rawlins JT, Dalley BK, Yang Q, Albertsen H*, et al.* Inhibition of DNA methyltransferase stimulates the expression of signal transducer and activator of transcription 1, 2, and 3 genes in colon tumor cells. Proc Natl Acad Sci U S A **1999**;96:14007-12

117. Matei D, Fang F, Shen C, Schilder J, Arnold A, Zeng Y*, et al.* Epigenetic resensitization to platinum in ovarian cancer. Cancer Res **2012**;72:2197-205

118. Chiappinelli KB, Strissel PL, Desrichard A, Li H, Henke C, Akman B*, et al.* Inhibiting DNA Methylation Causes an Interferon Response in Cancer via dsRNA Including Endogenous Retroviruses. Cell **2015**;162:974-86

119. Roulois D, Loo Yau H, Singhania R, Wang Y, Danesh A, Shen SY*, et al.* DNA-Demethylating Agents Target Colorectal Cancer Cells by Inducing Viral Mimicry by Endogenous Transcripts. Cell **2015**;162:961-73

120. Strick R, Strissel PL, Baylin SB, Chiappinelli KB. Unraveling the molecular pathways of DNA-methylation inhibitors: human endogenous retroviruses induce the innate immune response in tumors. Oncoimmunology **2016**;5:e1122160

121. Walsh CP, Chaillet JR, Bestor TH. Transcription of IAP endogenous retroviruses is constrained by cytosine methylation. Nat Genet **1998**;20:116-7

122. Chiappinelli KB, Zahnow CA, Ahuja N, Baylin SB. Combining Epigenetic and Immunotherapy to Combat Cancer. Cancer Res **2016**;76:1683-9

123. Katlinski KV, Gui J, Katlinskaya YV, Ortiz A, Chakraborty R, Bhattacharya S*, et al.* Inactivation of Interferon Receptor Promotes the Establishment of Immune Privileged Tumor Microenvironment. Cancer Cell **2017**;31:194-207

124.   Gao J, Shi LZ, Zhao H, Chen J, Xiong L, He Q, *et al.* Loss of IFN-gamma Pathway Genes in Tumor Cells as a Mechanism of Resistance to Anti-CTLA-4 Therapy. Cell **2016**;167:397-404 e9

125.   Benci JL, Xu B, Qiu Y, Wu TJ, Dada H, Twyman-Saint Victor C, *et al.* Tumor Interferon Signaling Regulates a Multigenic Resistance Program to Immune Checkpoint Blockade. Cell **2016**;167:1540-54 e12

126.   West AC, Mattarollo SR, Shortt J, Cluse LA, Christiansen AJ, Smyth MJ, *et al.* An intact immune system is required for the anticancer activities of histone deacetylase inhibitors. Cancer Res **2013**;73:7265-76

127.   Lisiero DN, Soto H, Everson RG, Liau LM, Prins RM. The histone deacetylase inhibitor, LBH589, promotes the systemic cytokine and effector responses of adoptively transferred CD8+ T cells. J Immunother Cancer **2014**;2:8

128.   Waibel M, Christiansen AJ, Hibbs ML, Shortt J, Jones SA, Simpson I, *et al.* Manipulation of B-cell responses with histone deacetylase inhibitors. Nat Commun **2015**;6:6838

129.   Kim K, Skora AD, Li Z, Liu Q, Tam AJ, Blosser RL, *et al.* Eradication of metastatic mouse cancers resistant to immune checkpoint blockade by suppression of myeloid-derived cells. Proc Natl Acad Sci U S A **2014**;111:11774-9

130.   Kopp LM, Ray A, Denman CJ, Senyukov VS, Somanchi SS, Zhu S, *et al.* Decitabine has a biphasic effect on natural killer cell viability, phenotype, and function under proliferative conditions. Mol Immunol **2013**;54:296-301

131.   Roby KF, Taylor CC, Sweetwood JP, Cheng Y, Pace JL, Tawfik O, *et al.* Development of a syngeneic mouse model for events related to ovarian cancer. Carcinogenesis **2000**;21:585-91

132.   Zhang L, Yang N, Garcia JR, Mohamed A, Benencia F, Rubin SC, *et al.* Generation of a syngeneic mouse model to study the effects of vascular endothelial growth factor in ovarian carcinoma. Am J Pathol **2002**;161:2295-309

133.   Conejo-Garcia JR, Benencia F, Courreges MC, Kang E, Mohamed-Hadley A, Buckanovich RJ, *et al.* Tumor-infiltrating dendritic cell precursors recruited by a beta-defensin contribute to vasculogenesis under the influence of Vegf-A. Nat Med **2004**;10:950-8

134.   Hung CF, Tsai YC, He L, Coukos G, Fodor I, Qin L, *et al.* Vaccinia virus preferentially infects and controls human and murine ovarian tumors in mice. Gene Ther **2007**;14:20-9

135.   Siegel RL, Miller KD, Jemal A. Cancer statistics, 2016. CA Cancer J Clin **2016**;66:7-30

136.   Vaughan S, Coward JI, Bast RC, Jr., Berchuck A, Berek JS, Brenton JD, *et al.* Rethinking ovarian cancer: recommendations for improving outcomes. Nat Rev Cancer **2011**;11:719-25

137.   Lee Y, Miron A, Drapkin R, Nucci MR, Medeiros F, Saleemuddin A, *et al.* A candidate precursor to serous carcinoma that originates in the distal fallopian tube. J Pathol **2007**;211:26-35

138.   Singh N, Gilks CB, Hirschowitz L, Kehoe S, McNeish IA, Miller D, *et al.* Primary site assignment in tubo-ovarian high-grade serous carcinoma: Consensus statement on unifying practice worldwide. Gynecol Oncol **2016**;141:195-8

139.   Flesken-Nikitin A, Hwang CI, Cheng CY, Michurina TV, Enikolopov G, Nikitin AY. Ovarian surface epithelium at the junction area contains a cancer-prone stem cell niche. Nature **2013**;495:241-5

140.   Kim J, Coffey DM, Ma L, Matzuk MM. The ovary is an alternative site of origin for high-grade serous ovarian cancer in mice. Endocrinology **2015**;156:1975-81

141. Howitt BE, Hanamornroongruang S, Lin DI, Conner JE, Schulte S, Horowitz N*, et al.* Evidence for a dualistic model of high-grade serous carcinoma: BRCA mutation status, histology, and tubal intraepithelial carcinoma. Am J Surg Pathol **2015**;39:287-93

142. Perets R, Wyant GA, Muto KW, Bijron JG, Poole BB, Chin KT*, et al.* Transformation of the fallopian tube secretory epithelium leads to high-grade serous ovarian cancer in Brca;Tp53;Pten models. Cancer Cell **2013**;24:751-65

143. Sherman-Baust CA, Kuhn E, Valle BL, Shih Ie M, Kurman RJ, Wang TL*, et al.* A genetically engineered ovarian cancer mouse model based on fallopian tube transformation mimics human high-grade serous carcinoma development. J Pathol **2014**;233:228-37

144. Walton J, Blagih J, Ennis D, Leung E, Dowson S, Farquharson M*, et al.* CRISPR/Cas9-Mediated Trp53 and Brca2 Knockout to Generate Improved Murine Models of Ovarian High-Grade Serous Carcinoma. Cancer Res **2016**;76:6118-29

145. Ricci F, Broggini M, Damia G. Revisiting ovarian cancer preclinical models: implications for a better management of the disease. Cancer Treat Rev **2013**;39:561-8

146. Hanahan D, Weinberg RA. Hallmarks of cancer: the next generation. Cell **2011**;144:646-74

147. Zhang L, Conejo-Garcia JR, Katsaros D, Gimotty PA, Massobrio M, Regnani G*, et al.* Intratumoral T cells, recurrence, and survival in epithelial ovarian cancer. N Engl J Med **2003**;348:203-13

148. Janat-Amsbury MM, Yockman JW, Anderson ML, Kieback DG, Kim SW. Comparison of ID8 MOSE and VEGF-modified ID8 cell lines in an immunocompetent animal model for human ovarian cancer. Anticancer Res **2006**;26:2785-9

149. Baert T, Verschuere T, Van Hoylandt A, Gijsbers R, Vergote I, Coosemans A. The dark side of ID8-Luc2: pitfalls for luciferase tagged murine models for ovarian cancer. J Immunother Cancer **2015**;3:57

150. Peter S, Bak G, Hart K, Berwin B. Ovarian tumor-induced T cell suppression is alleviated by vascular leukocyte depletion. Transl Oncol **2009**;2:291-9

151. Abiko K, Mandai M, Hamanishi J, Yoshioka Y, Matsumura N, Baba T*, et al.* PD-L1 on tumor cells is induced in ascites and promotes peritoneal dissemination of ovarian cancer through CTL dysfunction. Clin Cancer Res **2013**;19:1363-74

152. Duraiswamy J, Freeman GJ, Coukos G. Therapeutic PD-1 pathway blockade augments with other modalities of immunotherapy T-cell function to prevent immune decline in ovarian cancer. Cancer Res **2013**;73:6900-12

153. Wei H, Zhao L, Li W, Fan K, Qian W, Hou S*, et al.* Combinatorial PD-1 blockade and CD137 activation has therapeutic efficacy in murine cancer models and synergizes with cisplatin. PLoS One **2013**;8:e84927

154. Guo Z, Wang X, Cheng D, Xia Z, Luan M, Zhang S. PD-1 blockade and OX40 triggering synergistically protects against tumor growth in a murine model of ovarian cancer. PLoS One **2014**;9:e89350

155. Tsai HC, Li H, Van Neste L, Cai Y, Robert C, Rassool FV*, et al.* Transient low doses of DNA-demethylating agents exert durable antitumor effects on hematological and epithelial tumor cells. Cancer Cell **2012**;21:430-46

156. Weller EM, Poot M, Hoehn H. Induction of replicative senescence by 5-azacytidine: fundamental cell kinetic differences between human diploid fibroblasts and NIH-3T3 cells. Cell Prolif **1993**;26:45-54

157. Alexander VM, Roy M, Steffens KA, Kunnimalaiyaan M, Chen H. Azacytidine induces cell cycle arrest and suppression of neuroendocrine markers in carcinoids. Int J Clin Exp Med **2010**;3:95-102

158. Skelton D, Satake N, Kohn DB. The enhanced green fluorescent protein (eGFP) is minimally immunogenic in C57BL/6 mice. Gene Ther **2001**;8:1813-4

159. Challita PM, Kohn DB. Lack of expression from a retroviral vector after transduction of murine hematopoietic stem cells is associated with methylation in vivo. Proc Natl Acad Sci U S A **1994**;91:2567-71

160. Kuriyama S, Sakamoto T, Kikukawa M, Nakatani T, Toyokawa Y, Tsujinoue H*, et al.* Expression of a retrovirally transduced gene under control of an internal housekeeping gene promoter does not persist due to methylation and is restored partially by 5-azacytidine treatment. Gene Ther **1998**;5:1299-305

161. Kurman RJ, Shih Ie M. The origin and pathogenesis of epithelial ovarian cancer: a proposed unifying theory. Am J Surg Pathol **2010**;34:433-43

162. Kandalaft LE, Powell DJ, Jr., Singh N, Coukos G. Immunotherapy for ovarian cancer: what's next? J Clin Oncol **2011**;29:925-33

163. Nelson BH. New insights into tumor immunity revealed by the unique genetic and genomic aspects of ovarian cancer. Curr Opin Immunol **2015**;33:93-100

164. Chester C, Dorigo O, Berek JS, Kohrt H. Immunotherapeutic approaches to ovarian cancer treatment. J Immunother Cancer **2015**;3:7

165. Arrowsmith CH, Bountra C, Fish PV, Lee K, Schapira M. Epigenetic protein families: a new frontier for drug discovery. Nature reviews Drug discovery **2012**;11:384-400

166. Linnekamp JF, Butter R, Spijker R, Medema JP, van Laarhoven HW. Clinical and biological effects of demethylating agents on solid tumours - A systematic review. Cancer Treat Rev **2017**;54:10-23

167. Henke C, Ruebner M, Faschingbauer F, Stolt CC, Schaefer N, Lang N*, et al.* Regulation of murine placentogenesis by the retroviral genes Syncytin-A, Syncytin-B and Peg10. Differentiation **2013**;85:150-60

168. Henke C, Strissel PL, Schubert MT, Mitchell M, Stolt CC, Faschingbauer F*, et al.* Selective expression of sense and antisense transcripts of the sushi-ichi-related retrotransposon--derived family during mouse placentogenesis. Retrovirology **2015**;12:9

169. Swann JB, Hayakawa Y, Zerafa N, Sheehan KC, Scott B, Schreiber RD*, et al.* Type I IFN contributes to NK cell homeostasis, activation, and antitumor function. J Immunol **2007**;178:7540-9

170. Ross SM. Peirce's criterion for the elimination of suspect experimental data. Journal of Engineering Technology **2003**;20:38-41

171. Ostrand-Rosenberg S, Sinha P. Myeloid-derived suppressor cells: linking inflammation and cancer. J Immunol **2009**;182:4499-506

172. Bingle L, Brown NJ, Lewis CE. The role of tumour-associated macrophages in tumour progression: implications for new anticancer therapies. J Pathol **2002**;196:254-65

173. Shultz LD, Ishikawa F, Greiner DL. Humanized mice in translational biomedical research. Nat Rev Immunol **2007**;7:118-30

174. Mikula-Pietrasik J, Uruski P, Szubert S, Moszynski R, Szpurek D, Sajdak S*, et al.* Biochemical composition of malignant ascites determines high aggressiveness of undifferentiated ovarian tumors. Med Oncol **2016**;33:94

175. Carr MW, Roth SJ, Luther E, Rose SS, Springer TA. Monocyte chemoattractant protein 1 acts as a T-lymphocyte chemoattractant. Proc Natl Acad Sci U S A **1994**;91:3652-6

176. Xu LL, Warren MK, Rose WL, Gong W, Wang JM. Human recombinant monocyte chemotactic protein and other C-C chemokines bind and induce directional migration of dendritic cells in vitro. J Leukoc Biol **1996**;60:365-71

177. Dufour JH, Dziejman M, Liu MT, Leung JH, Lane TE, Luster AD. IFN-gamma-inducible protein 10 (IP-10; CXCL10)-deficient mice reveal a role for IP-10 in effector T cell generation and trafficking. J Immunol **2002**;168:3195-204

178. Fresco R, Glaspy J, Palodichuk C. 2016 Phase II Randomized Study of Pembrolizumab With or Without Epigenetic Modulation With CC-486 in Patients With Platinum-resistant Epithelial Ovarian, Fallopian Tube or Primary Peritoneal Cancer, NCT02900560. Bethesda (MD): National Library of Medicine (US). Accessed 2016.

MEREDITH L. STONE

716.361.8681 • mstone14@jhmi.edu

EDUCATION

❖ **JOHNS HOPKINS UNIVERSITY SCHOOL OF MEDICINE**
    Baltimore, MD
– Ph.D. candidate in Cellular and Molecular Medicine   *2012-March 2017*
– Course work: Human Body: Anatomy, Physiology, & Histology; Molecular Biology;
Genetics; Pathways & Regulation; Cell Structure & Dynamics; Cellular & Molecular
Basis of Disease; Immunology; Grant Writing; Drug Discovery Research; New
Approaches to Cancer Prevention & Therapy; Fundamentals of Cancer: Cause to
Cure; Statistics for Laboratory Scientists.

❖ **CORNELL UNIVERSITY**– College of Agriculture and Life Sciences   Ithaca, NY
– B.S. in Biological Sciences - 3.42 GPA (Three year graduate)   *2009- 2012*

❖ **NARDIN ACADEMY**   Buffalo, NY
– Class of 2009. 4.0 GPA.   *2005 - 2009*

RESEARCH EXPERIENCE

❖ **JOHNS HOPKINS SCHOOL OF MEDICINE**
Baltimore, MD
Cynthia Zahnow and Stephen Baylin- Thesis Advisors   *2013-present*
    – Sidney Kimmel Comprehensive Cancer Center, Department of Oncology,
     Cancer Biology Research Program.
    – Thesis Project: Combination epigenetic therapy directly affects tumor cells to
      sensitize an ovarian cancer mouse model to immune checkpoint therapy.
        • Using a syngeneic mouse model, we have shown that through direct
          actions on ovarian cancer cells, the demethylating agent 5-azacytidine
          has an antitumorigenic effect in mice, as well as inducing immune cell
          recruitment to the tumor microenvironment.
        • Furthermore, we have shown that when the demethylating agent is
          combined with a histone deacetlylase inhibitor, mice have decreased
          tumor burden and increased survival in an immune competent model but
          not an immunodeficient model, suggesting that the efficacy of the
          combination epigenetic therapy is in part due to the effect of the drugs on
          the tumor microenvironment.
        • Finally, when anti-PD-1 immune checkpoint therapy is added to the
          combination *epigenetic* therapy, there are significant increases in the
          activation of the immune cells recruited to the tumor microenvironment,
          correlating with improved survival of the mice.
      – Mentorship: I trained one graduate rotation student who went on to join the lab.
      I also managed and guided one undergraduate student during a summer
      research project.
      – Reviewed a manuscript for *Integrative Cancer Biology and Research*

❖ **CORNELL UNIVERSITY**
Ithaca, NY *Alexander Nikitin – Department of Biomedical Sciences*   *2010-2012*
    – Utilized prostatasphere assays and immunostaining to characterize mouse
      prostate stem cell activity and the protein levels of the targets of the mir34 family
      of microRNAs.

❖ **ROSWELL PARK CANCER INSTITUTE**
Buffalo, NY *Kenneth W. Gross – Department of Cancer Genetics*
Summer 2010
– Extracted DNA from and genotyped ~100 mice per week with PCR,
  characterized tumors with ELISA assays, and performed lab maintenance.
Andrei V. Bakin – Department of Cancer Genetics
  Summer 2008
– Roswell Park Cancer Institute Research Participation Program for Young
  Scholars – presented a poster titled "Construction of epithelial cells expressing
  mJunB cDNA under control of the Tet-off system."

PAPERS

Under review at *Cancer Research*: **Meredith L. Stone**, Katherine B. Chiappinelli, Huili
Li, Lauren Murphy, Meghan Travers, Michael Topper, Dimitris Mathios, Michael Lim,
Tian-Li Wang, Chien Fu Hung, Stephen B. Baylin, and Cynthia A. Zahnow*.
Combination epigenetic therapy regulates tumor cells and the immune
microenvironment to sensitize an ovarian cancer mouse model to immune
checkpoint therapy.*

C.A*.* Zahnow, M. Topper, **M. Stone**, T. Murray-Stewart, H. Li, S.B. Baylin, R.A. Casero
Jr. Inhibitors of DNA Methylation, Histone Deacetylation, and Histone Demethylation:
A Perfect Combination for Cancer Therapy. *Advances in Cancer Research* 130:55-
111 (2016).

INVITED TALKS

Stone, Meredith; Chiappinelli, Katherine; Li, Huili; Murphy, Lauren; Topper, Michael;
Mathios, Dimitris; Lim, Michael; Baylin, Stephen; and Zahnow, Cynthia*.* "Epigenetic
treatment of ovarian cancer cells increases immune cell recruitment: Implications for
response to immune checkpoint therapy."   *AACR Advances in Ovarian Cancer
Research,* Orlando, FL. (October, 2015)

POSTERS AND PRESENTATIONS

Stone, Meredith; Chiappinelli, Katherine; Li, Huili; Murphy, Lauren; Topper, Michael;
Mathios, Dimitris; Lim, Michael; Baylin, Stephen; and Zahnow, Cynthia. "Epigenetic
treatment of ovarian cancer cells increases immune cell recruitment: Implications for
response to immune checkpoint therapy."   *AACR Annual Meeting,* New Orleans,
LA. (April, 2016).

Stone, Meredith; Chiappinelli, Katherine; Li, Huili; Murphy, Lauren; Topper, Michael;
Mathios, Dimitris; Lim, Michael; Baylin, Stephen; and Zahnow, Cynthia. "Epigenetic
treatment of ovarian cancer cells increases immune cell recruitment: Implications for
response to immune checkpoint therapy." *Sidney Kimmel Comprehensive Cancer
Center Annual Fellows Research Day,* Baltimore, MD (May, 2015).

Stone, Meredith; Chiappinelli, Katherine; Li, Huili; Baylin, Stephen; and Zahnow,
Cynthia*.* "Epigenetics: A new approach to anti-tumor immune activation therapy."
Cellular and Molecular Medicine Graduate Program Annual Retreat, Baltimore, MD
(September, 2014).

Stone, Meredith; Chung, Jon; Bunz, Fred. "A potential mediator of p53 dependent
apoptosis." *Cellular and Molecular Medicine Rotation Presentations,* Baltimore, MD
(May, 2013).

Stone, Meredith; Miles, Linde; Poirier, John; Rudin, Charles. " Evaluation of the SVV
3C protease in cleaving optimized substrates during a cellular SVV infection."

Cellular and Molecular Medicine Rotation Presentations, Baltimore, MD (December, 2012).

Hwang, Chang-il; Cheng, Chieh-Yang; Corney, David; **Stone, Meredith**; Korner, Stephanie; Munroe, Robert; Schimenti, John C.; Hermeking, Heiko; Nikitin, Alexander Yu. "miR-34 roles in regulation of normal and neoplastic stem cells of the prostate epithelium." *Cornell University Stem Cell Program Retreat*, Ithaca, NY (September, 2011).

Stone, Meredith; Gervasi, Megan; Bakin, Andrei. "Construction of epithelial cells expressing mJunB cDNA under control of the Tet-off System." *Roswell Park Research Program for Young Scholars*, Buffalo, NY (August, 2008).

TECHNICAL SKILLS

– *In vivo:* Mouse handling, tumor xenograft and syngeneic models, drug preparation and injection (intraperitoneal and subcutaneous), mouse dissection and tissue collection (including ascites fluid and bone marrow), preparation of tissue for flow cytometry, tissue fixation.

– *In vitro:* Cell culture, flow cytometry, cell cycle, apoptosis, and senescence assays, western blotting, qRTPCR, fluorescent microscopy, DNA and RNA extraction, PCR and gel electrophoresis, sphere assays in methylcellulose, hematoxylin and eosin staining, and immunohistochemistry.

HONORS AND AWARDS

– Cornell Undergraduate Stem Cell Science Program (2011)- Chosen as one of eight students to participate; attended the Cornell Stem Cell Retreat and presented my findings; sponsored to attend the Annual Biomedical Research Conference for Minority Students in St. Louis, MO. (November, 2011).

– AP Scholar with Honor (2009)

– *Business First's* All-Western New York First Academic Team (2009)

– Bausch and Lomb Science Scholarship (2009)

– Roswell Park Cancer Institute Research Participation Program for Young Scholars (2008)- selected as a high school student to participate in RPCI's competitive summer research program.

– National Merit Scholarship Winner (2008)

SCIENCE OUTREACH

– Stand Up to Cancer: Mentored and trained a recipient of the Emperor Science Award for high school students (2016).

–STEM night at Henderson-Hopkins School- taught middle school age kids how to perform a DNA extraction (2016).

REFERENCES

Thesis advisor:
Dr. Cynthia Zahnow, Ph.D.
Associate Professor of Oncology
Department of Oncology
The Sidney Kimmel Cancer Center at Johns Hopkins University
Phone: (410) 955-8506
Email: zahnoci@jhmi.edu

Thesis advisor:
Dr. Stephen B. Baylin, M.D.

Virginia and D.K. Ludwig Professor for Cancer Research
Department of Oncology
The Sidney Kimmel Cancer Center at Johns Hopkins University
Phone: (410) 955-8506
Email: sbaylin@jhmi.edu

Thesis Committee Chair
Dr. Robert A. Casero, Jr.
Professor of Oncology
Department of Oncology
The Sidney Kimmel Cancer Center at Johns Hopkins University
Phone: (410) 955-8580
Email: rcasero@jhmi.edu